A coupled boundary element / finite element method for the convected Helmholtz equation with non-uniform flow in a bounded domain

Fabien Casenave[1,2], Alexandre Ern[1] and Guillaume Sylvand[2]

[1] Université Paris-Est, CERMICS (ENPC), 6-8 Avenue Blaise Pascal, Cité Descartes, F-77455 Marne-la-Vallée, France
[2] EADS-IW, 18 rue Marius Terce, 31300 Toulouse, France

March 28, 2013

Abstract

We consider linear acoustic propagation at a fixed frequency in a subsonic convective flow around a scattering object, under the assumption that the flow is uniform far away from the object. Using the Prandtl–Glauert transformation, the convected Helmholtz equation yields the classical Helmholtz equation in the exterior domain where the flow is uniform. We then derive two coupled methods to solve the problem approximately using the finite element method in the interior domain around the scattering object and the boundary element method on the coupling surface with the exterior domain. The first one admits infinitely many solutions at resonant frequencies. The second one is based on the combined field integral equations method, and is well-posed at all frequencies. We perform the analysis of the two formulations and present numerical results illustrating the advantages of the second formulation.

1 Introduction

The scope of the present work is the computation of linear acoustic wave propagation at a fixed frequency in the presence of a flow. The simplest model is the Helmholtz equation, when the flow is at rest. When the medium of propagation is not at rest, the governing equation is a convected Helmholtz equation resulting from the linearized harmonic Euler equations. The numerical method we propose hinges on the linearity of the convected Helmholtz equation. Therefore, nonlinear interaction between acoustics and fluid mechanics phenomena is not considered; we refer to the early work of Lighthill for aerodynamically generated acoustic sources [29, 30], to [21] for a review on nonlinear acoustics, and to [38] for the coupling of Computational Aero Acoustic (CAA) and Computational Fluid Dynamics (CFD) solvers.

Our main assumption on the flow is that it is irrotational close to the scattering object and uniform far away from it. This geometric setup leads to a partition of the unbounded medium of propagation into two subdomains, the bounded interior domain near the scattering object where the flow is non-uniform and the unbounded exterior domain far away from the object where the flow is uniform. A convenient tool to handle the convected Helmholtz equation is the Prandtl–Glauert transformation, which was used in [14] in the case of globally uniform and subsonic flow. Our first contribution is the extension of this transformation to the case of non-uniform flow in the interior domain, still under the assumption that the convective flow is everywhere subsonic. In particular, the transformed convected Helmholtz equation simplifies into the classical Helmholtz equation in the exterior domain, and in the interior domain, leads to an anisotropic definite positive diffusive matrix and a skew-symmetric first-order term. Our second contribution is to derive and analyze a mathematically well-posed numerical method to approximate the transformed convected Helmholtz equation uniformly at all frequencies. Numerical methods for acoustic scattering include infinite finite elements [40, 3], the method of fundamental solutions [17], and the retarded potential method [15, 36].

In the case of the Helmholtz equation, the problem of acoustic scattering by a solid object can be reduced to finding unknown functions defined on its surface and which solve integral equations. The boundary element method (BEM) is then used to approximate these equations numerically [35]. When the medium of propagation is non-uniform or when there is a non-uniform flow around the scattering object, a volumic resolution has to be considered, e.g. using a finite element method (FEM). If such non-uniformities occur only in a given bounded domain, it is possible to benefit from the advantages of both a volumic resolution and an integral equation formulation. Coupling BEM and FEM at the boundary of the given bounded domain allows this. Coupled BEM-FEM can be traced back to Zienkiewicz, Kelly and Bettess in 1977 [4], and Johnson and Nédélec in 1980 [25]. These methods have been applied to Maxwell equations [28]. In what follows, we first derive an unstable coupled formulation which is well-posed except at resonant frequencies for which it leads to infinitely many solutions. All these solutions deliver the same acoustic potential in the exterior domain, but because of the lack of uniqueness, the numerical procedure becomes ill-conditioned. This problem has been tackled in [7, 22], where a stabilization of the coupling, based on combined field integral equations, has been proposed in the zero flow case by means of introducing an additional unknown at the coupling surface. Using a similar stabilization method, we derive a stable coupled formulation for the convected Helmholtz equation. This formulation is well-posed at all frequencies. Our numerical results show that the unstable formulation yields results polluted by spurious oscillations in the close vicinity of resonant frequencies, whereas the stable formulation yields consistent solutions at all frequencies. This advantage of the stable formulation is particularly relevant in practice at high frequencies, where the density of resonant frequencies is higher.

The material is organized as follows: the problem of interest is presented in Section 2, and coupling procedures are detailed in Section 3, where the main mathematical results are stated. The finite-dimensional approximation of the formulations is addressed in Section 4. Finally, numerical results are presented in Section 5, and some conclusions are drawn in Section 6. In Appendix A, some details are given on the application of the Prandtl–Glauert transformation to the convected Helmholtz equation. The proofs of the mathematical results are presented in Appendix B.

2 Aeroacoustic problem

This section describes the problem of acoustic scattering by a solid object in a non-uniform convective flow, together with the underlying physical assumptions.

2.1 Notation and preliminaries

Figure 1 describes the geometric setup. The interior domain, corresponding to the area near the scattering object where the convective flow is non-uniform, is denoted by Ω^-. In the exterior domain, Ω^+, the convective flow is assumed to be uniform. The complete medium of propagation, denoted by $\Omega \subset \mathbb{R}^3$, is such that $\Omega := \Omega^+ \cup \Omega^- \cup \Gamma_\infty = \mathbb{R}^3 \backslash \{\text{solid object}\}$, where $\Gamma_\infty := \partial\Omega^+ \cap \partial\Omega^-$ is the boundary between the interior and exterior domains. The surface Γ_∞ is assumed to be Lipschitz. Such an assumption is sufficiently large to include for instance polyhedric surfaces resulting from the use of a finite element mesh in Ω^-. The surface of the solid scattering object, $\partial\Omega^- \backslash \Gamma_\infty$, is denoted by Γ and is assumed to be Lipschitz.

The speed of sound when the medium of propagation is at rest is denoted by c, the wave number by k, the density by ρ, and the acoustic velocity and pressure, respectively, by $\boldsymbol{v}$ and p. The rescaled velocity is defined as $\boldsymbol{M} := c^{-1}\boldsymbol{v}$, where $M := |\boldsymbol{M}|$ is the Mach number. The subscript ∞ refers to uniform flow quantities related to Ω^+, whereas the subscript 0 refers to point-dependent flow quantities related to Ω^-, that is, $\rho_{|\Omega^-} = \rho_0(\boldsymbol{x})$, $\rho_{|\Omega^+} \equiv \rho_\infty$, $k_{|\Omega^-} = k_0(\boldsymbol{x})$, $k_{|\Omega^+} \equiv k_\infty$, $c_{|\Omega^-} = c_0(\boldsymbol{x})$, $c_{|\Omega^+} \equiv c_\infty$, $\boldsymbol{M}_{|\Omega^-} = \boldsymbol{M}_0(\boldsymbol{x})$, $\boldsymbol{M}_{|\Omega^+} \equiv \boldsymbol{M}_\infty$. The convective flow is continuous through Γ_∞ and tangential on Γ. Hence ρ, k and $\boldsymbol{M}$ are continuous through Γ_∞, and $\boldsymbol{M} \cdot \boldsymbol{n} = 0$ on Γ.

The source term g is time-harmonic with pulsation ω and is assumed to be located at Ω^+ for simplicity. This source term is an acoustic monopole located in $x_s \in \Omega^+$ of amplitude A_s, so that $\hat{g} := A_s \delta_{x_s} \cos(\omega t)$, where δ denotes the Dirac mass distribution. The physical quantities are associated with complex quantities with the following convention on, for instance, the acoustic pressure:

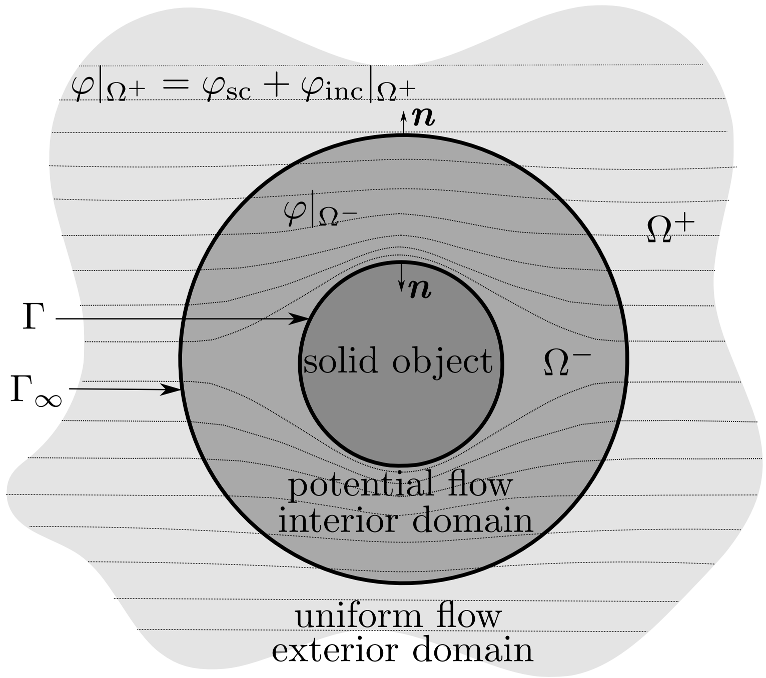

Figure 1: Geometric setup for the coupled problem

$p \leftrightarrow \mathrm{Re}\,(p \exp(-i\omega t))$. In what follows, we always refer to the complex quantity. Furthermore, the Hermitian product of two vectors $\boldsymbol{U}, \boldsymbol{W} \in \mathbb{C}^3$ is denoted by $\overline{\boldsymbol{U}} \cdot \boldsymbol{W} := \sum_{i=1}^{3} \overline{U_i} W_i$, where $\bar{\cdot}$ denotes the complex conjugate, and the associated Euclidian norm in $\mathbb{C}^3$ is denoted by $\|\cdot\|$.

2.2 The convected Helmholtz equation

In the interior domain Ω^-, the convective flow is supposed to be stationary, inviscid, isentropic, irrotational and subsonic. The acoustic effects are considered to be a first-order perturbation of this flow. With these assumptions, the acoustic velocity $\boldsymbol{v}$ is irrotational, so that there exists an acoustic potential φ such that $\boldsymbol{v} = \boldsymbol{\nabla}\varphi$.

Following [23, Equation (F27)] and [20], and making use of the irrotationality of the convective flow, the linearization of the Euler equations leads to

$$\rho\left(k^2\varphi + ik\boldsymbol{M}\cdot\boldsymbol{\nabla}\varphi\right) + \boldsymbol{\nabla}\cdot\left(\rho\left(\boldsymbol{\nabla}\varphi - \left(\boldsymbol{M}\cdot\boldsymbol{\nabla}\varphi\right)\boldsymbol{M} + ik\varphi\boldsymbol{M}\right)\right) = g \quad \text{in } \Omega, \tag{1}$$

where φ is the unknown acoustic potential, and ρ, k, $\boldsymbol{M}$, and $g = A_s\delta_{x_s}$ are known. Equation (1) is the convected Helmholtz equation. Under the assumption that the acoustic perturbations are perfectly reflected by the solid object, the acoustic potential verifies an homogeneous Neumann boundary condition on Γ:

$$\boldsymbol{\nabla}\varphi\cdot\boldsymbol{n} = 0 \quad \text{on } \Gamma. \tag{2}$$

Problem (1)-(2) is completed by a Sommerfeld-like boundary condition at infinity (see (12c) below) that selects outgoing waves to ensure uniqueness of the solution. In the exterior domain Ω^+ where the flow quantities are uniform, equation (1) simplifies into

$$\Delta\varphi + k_\infty^2\varphi + 2ik_\infty\boldsymbol{M}_\infty\cdot\boldsymbol{\nabla}\varphi - \boldsymbol{M}_\infty\cdot\boldsymbol{\nabla}\left(\boldsymbol{M}_\infty\cdot\boldsymbol{\nabla}\varphi\right) = g \quad \text{in } \Omega^+. \tag{3}$$

If there were no scattering object and if the convective flow were uniform in $\mathbb{R}^3$ (and thus equal to the flow at infinity), the source term g would create an acoustic potential denoted by $\varphi_{\rm inc}$ in $\mathbb{R}^3$. This potential, which solves (3) in $\mathbb{R}^3$, has an analytical expression, and $\varphi_{\rm inc}$ and $\boldsymbol{n}\cdot\boldsymbol{\nabla}\varphi_{\rm inc}$ are continuous across Γ_∞. The acoustic potential scattered by the solid object is defined as $\varphi_{\rm sc} := \varphi - \varphi_{\rm inc}$ in Ω^+. Eliminating the known acoustic potential $\varphi_{\rm inc}$ created by the source yields

$$\Delta\varphi_{\rm sc} + k_\infty^2\varphi_{\rm sc} + 2ik_\infty\boldsymbol{M}_\infty\cdot\boldsymbol{\nabla}\varphi_{\rm sc} - \boldsymbol{M}_\infty\cdot\boldsymbol{\nabla}\left(\boldsymbol{M}_\infty\cdot\boldsymbol{\nabla}\varphi_{\rm sc}\right) = 0 \quad \text{in } \Omega^+. \tag{4}$$

2.3 The Prandtl–Glauert transformation

The Prandtl–Glauert transformation was introduced by Glauert in 1928 [19] to study the compressible effects of the air on the lift of an airfoil and was applied to subsonic aeroacoustic problems by Amiet and Sears in 1970 [1]. Herein, the Prandtl–Glauert transformation is applied in the complete medium of propagation and is based on the reduced velocity $\boldsymbol{M}_\infty$. This transformation consists in changing the space and time variables as

$$\begin{cases} \boldsymbol{x}' = \gamma_\infty \left(\hat{\boldsymbol{M}}_\infty \cdot \boldsymbol{x}\right) \hat{\boldsymbol{M}}_\infty + \left(\boldsymbol{x} - (\hat{\boldsymbol{M}}_\infty \cdot \boldsymbol{x})\hat{\boldsymbol{M}}_\infty\right) & \boldsymbol{x} \in \Omega, \\ t' = t - \dfrac{\gamma_\infty^2}{c_\infty}\boldsymbol{M}_\infty \cdot \boldsymbol{x} & t \in \mathbb{R}, \end{cases} \tag{5}$$

where $\gamma_\infty := \frac{1}{\sqrt{1-M_\infty^2}}$ and $\hat{\boldsymbol{M}}_\infty := M_\infty^{-1}\boldsymbol{M}_\infty$ with $M_\infty := |\boldsymbol{M}_\infty|$. The spatial transformation corresponds to a dilatation along $\hat{\boldsymbol{M}}_\infty$ of magnitude γ_∞, the component orthogonal to $\hat{\boldsymbol{M}}_\infty$ being unchanged. In what follows, we suppose that $M_\infty < 1$, so that the Prandtl–Glauert transformation is a $\mathcal{C}^\infty$-diffeomorphism from $\Omega \times \mathbb{R}$ to $\Omega' \times \mathbb{R}$, where Ω' denotes the transformed medium of propagation.

2.4 The transformed problem

Let f be such that $\varphi(\boldsymbol{x}) = f(\boldsymbol{x}')\exp\left(-ik_\infty\gamma_\infty\left(\boldsymbol{M}_\infty \cdot \boldsymbol{x}'\right)\right)$, $\boldsymbol{x}' \in \Omega'$; f_{inc} and f_{sc} are defined from φ_{inc} and φ_{sc} in the same fashion, so that f_{inc} is analytically known, and defined in $\mathbb{R}^3$. Let $\varsigma(\boldsymbol{x}') := \rho_\infty^{-1}\exp\left(ik_\infty\gamma_\infty\left(\boldsymbol{M}_\infty \cdot \boldsymbol{x}'\right)\right)g(\boldsymbol{x}')$, $\boldsymbol{x}' \in \Omega'$.

In what follows, the transformed geometry, unknowns and operators are considered unless specified otherwise. For brevity, primes are omitted. The convected Helmholtz equation (1) after the Prandtl–Glauert transformation becomes

$$rk^2\beta f + irk\boldsymbol{V}\cdot\boldsymbol{\nabla} f + \boldsymbol{\nabla}\cdot\left(irkf\boldsymbol{V} + r\Xi\boldsymbol{\nabla} f\right) = \varsigma \quad \text{in } \Omega, \tag{6}$$

while the boundary condition (2) becomes

$$\left(irkf\boldsymbol{V} + r\Xi\boldsymbol{\nabla} f\right)\cdot\boldsymbol{n} = 0 \quad \text{on } \Gamma, \tag{7}$$

where $r := \frac{\rho}{\rho_\infty}$, $\beta := (1+qP)^2 - q^2M_\infty^2$, $\boldsymbol{V} := (1+qP)\mathcal{N}\boldsymbol{M} - q\gamma_\infty\boldsymbol{M}_\infty$, $q := \gamma_\infty^2\frac{k_\infty}{k}$, $P := \boldsymbol{M}\cdot\boldsymbol{M}_\infty$ and $\Xi := \mathcal{N}\mathcal{O}\mathcal{N}$ with $\mathcal{N} := I + C_\infty\boldsymbol{M}_\infty\boldsymbol{M}_\infty^T$, $\mathcal{O} := I - \boldsymbol{M}\boldsymbol{M}^T$, and $C_\infty := \frac{\gamma_\infty - 1}{M_\infty^2}$. The derivation of equations (6)-(7) is sketched in Appendix A. An important observation is that in Ω^+, $\beta = \gamma_\infty^2$, $\boldsymbol{V} = \boldsymbol{0}$ and $\Xi = I$, so that (6) becomes

$$\Delta f + \hat{k}_\infty^2 f = \varsigma \quad \text{in } \Omega^+, \tag{8}$$

where $\hat{k}_\infty := \gamma_\infty k_\infty$. Moreover, since $\text{supp}(\varsigma) \subset \Omega^+$, f_{inc} satisfies

$$\Delta f_{\text{inc}} + \hat{k}_\infty^2 f_{\text{inc}} = \varsigma \quad \text{in } \Omega^+, \qquad \Delta f_{\text{inc}} + \hat{k}_\infty^2 f_{\text{inc}} = 0 \quad \text{in } \mathbb{R}^3\backslash\Omega^+. \tag{9}$$

Eliminating f_{inc} in (8) yields,

$$\Delta f_{\text{sc}} + \hat{k}_\infty^2 f_{\text{sc}} = 0 \quad \text{in } \Omega^+. \tag{10}$$

This is the classical Helmholtz equation with modified wave number $\hat{k}_\infty$. Another important property is that the matrix Ξ is symmetric positive definite in Ω^- as well. Indeed, there holds in Ω^-,

$$\overline{\boldsymbol{U}}\cdot\Xi\boldsymbol{U} \geq \left(1 - M_0^2\right)\|\boldsymbol{U}\|^2 \ \text{ for all } \boldsymbol{U} \in \mathbb{C}^3, \tag{11}$$

where M_0 is uniformly bounded away from 1 since the convective flow is assumed to be subsonic. Moreover, for all $\boldsymbol{U}, \boldsymbol{W} \in \mathbb{C}^3$, there holds $\overline{\boldsymbol{U}}\cdot\Xi\boldsymbol{W} \leq \frac{1+M_0^2}{1-M_\infty^2}\|\boldsymbol{U}\|\|\boldsymbol{W}\|$ in Ω^-.

In summary, the boundary value problem we consider is

$$rk^2\beta f + irk\boldsymbol{V}\cdot\boldsymbol{\nabla} f + \boldsymbol{\nabla}\cdot\left(irkf\boldsymbol{V} + r\Xi\boldsymbol{\nabla} f\right) = \varsigma \quad \text{in } \Omega, \tag{12a}$$

$$\left(irkf\boldsymbol{V} + r\Xi\boldsymbol{\nabla} f\right)\cdot\boldsymbol{n} = 0 \quad \text{on } \Gamma, \tag{12b}$$

$$\lim_{r\to+\infty} r\left(\frac{\partial(f - f_{\text{inc}})}{\partial r} - i\hat{k}_\infty(f - f_{\text{inc}})\right) = 0, \tag{12c}$$

where f is searched in $H^1_{\mathrm{loc}}(\Omega) := \{u \in H^1(K), \forall K \subset \Omega \text{ compact}\}$. Equation (12a) is the transformed convected Helmholtz equation, (12b) the transformed boundary condition, and the condition at infinity (12c) the classical Sommerfeld radiation condition that guarantees existence and uniqueness for Helmholtz exterior problems [31, Theorem 9.10]. In the general case, the Sommerfeld radiation condition is written for the scattered potential, since some incident acoustic potentials, e.g., plane waves, do not verify it.

3 Coupling procedure

Problem (12) is separated into an interior problem posed in Ω^- and an exterior problem posed in Ω^+ in view of using different numerical methods in each subdomain. Specifically, the problem in the interior domain is solved by means of finite elements, whereas the problem in the exterior domain is solved by means of boundary elements. The main purpose of this section is to derive two coupling procedures between the interior and exterior problems.

3.1 The transmission problem

The one-sided Dirichlet traces on Γ_∞ of a smooth function u in $\Omega^+ \cup \Omega^-$ are defined as $\gamma_0^\pm u^\pm := u^\pm|_{\Gamma_\infty}$, and the one-sided Neumann traces as $\gamma_1^\pm u^\pm := (\boldsymbol{\nabla} u^\pm)|_{\Gamma_\infty} \cdot \boldsymbol{n}$, where $u^\pm := u|_{\Omega^\pm}$ and where $\boldsymbol{n}$ is the unit normal vector to Γ_∞ conventionally pointing towards Ω^+ (see Figure 1). The one-sided normal traces on Γ_∞ of a smooth vector field $\boldsymbol{\sigma}$ in $\Omega^+ \cup \Omega^-$ are defined as $\gamma_n^\pm \boldsymbol{\sigma}^\pm := \boldsymbol{\sigma}^\pm|_{\Gamma_\infty} \cdot \boldsymbol{n}$, where $\boldsymbol{\sigma}^\pm := \boldsymbol{\sigma}|_{\Omega^\pm}$. These trace operators are extended to bounded linear operators $\gamma_0^\pm : H^1(\Omega^\pm) \to H^{\frac{1}{2}}(\Gamma_\infty)$, $\gamma_1^\pm : H(\Delta, \Omega^\pm) \to H^{-\frac{1}{2}}(\Gamma_\infty)$ and $\gamma_n^\pm : H(\mathrm{div}, \Omega^\pm) \to H^{-\frac{1}{2}}(\Gamma_\infty)$, where $H^1(\Omega^\pm)$, $H^{\frac{1}{2}}(\Gamma_\infty)$, and $H^{-\frac{1}{2}}(\Gamma_\infty)$ are the usual Sobolev spaces on $\Omega^\pm$ and Γ_∞, $H(\mathrm{div}, \Omega^\pm) = \{\boldsymbol{\sigma} \in \mathrm{L}^2(\Omega^\pm), \boldsymbol{\nabla} \cdot \boldsymbol{\sigma} \in \mathrm{L}^2(\Omega^\pm)\}$, with $L^2(\Omega^\pm)$ the Lebesgue space of square integrable functions on $\Omega^\pm$, and $H(\Delta, \Omega^\pm) = \{u^\pm \in H^1(\Omega^\pm), \Delta u^\pm \in L^2(\Omega^\pm)\}$ (see [37, Lemma 20.2]). It is actually sufficient to consider functional spaces on compact subsets of Ω^+ to define exterior traces on Γ_∞. Let X denote the surface Γ or Γ_∞. The $L^2(X)$-inner product $(\cdot,\cdot) : L^2(X) \times L^2(X) \to \mathbb{C}$ is defined as

$$(\lambda, \mu)_X := \int_X \overline{\lambda}(\boldsymbol{y}) \mu(\boldsymbol{y}) ds(\boldsymbol{y}). \tag{13}$$

This inner product can be extended to a duality pairing on $H^{-\frac{1}{2}}(X) \times H^{\frac{1}{2}}(X)$.

We consider the following transmission problem where the one-sided normal trace $\gamma_{n,\Gamma}^-$ on Γ from Ω^- is used to formulate the boundary condition (12b):

$$rk^2\beta f^- + irk\boldsymbol{V} \cdot \boldsymbol{\nabla} f^- + \boldsymbol{\nabla} \cdot (irkf\boldsymbol{V} + r\Xi\boldsymbol{\nabla} f)^- = 0 \quad \text{in } \Omega^-, \tag{14a}$$

$$\Delta f_{\mathrm{sc}} + \hat{k}_\infty^2 f_{\mathrm{sc}} = 0 \quad \text{in } \Omega^+, \tag{14b}$$

$$\gamma_{n,\Gamma}^- (irkf\boldsymbol{V} + r\Xi\boldsymbol{\nabla} f)^- = 0 \quad \text{on } \Gamma, \tag{14c}$$

$$\gamma_0^+ f^+ - \gamma_0^- f^- = 0 \quad \text{on } \Gamma_\infty, \tag{14d}$$

$$\gamma_1^+ f^+ - \gamma_1^- f^- = 0 \quad \text{on } \Gamma_\infty, \tag{14e}$$

$$\lim_{r\to+\infty} r \left(\frac{\partial(f^+ - f^+_{\mathrm{inc}})}{\partial r} - i\hat{k}_\infty (f^+ - f^+_{\mathrm{inc}}) \right) = 0. \tag{14f}$$

Proposition 3.1. *Problem* (12) *is equivalent to Problem* (14).

Proof. If f solves (12), it is clear that f solves (14). Conversely, let f be defined in $\Omega^+ \cup \Omega^-$ such that f verifies (14). From [31, Lemma 4.19], since f solves (14a) and (14b), then f solves (12a) if and only if the jumps on Γ_∞ of its traces and of the normal component of $irkf\boldsymbol{V} + r\Xi\boldsymbol{\nabla} f$ vanish. The first condition is just (14d), while the second condition is $\gamma_1^+ f^+ - \gamma_n^- (irkf\boldsymbol{V} + r\Xi\boldsymbol{\nabla} f)^- = 0$, which, by continuity of the convective flow across Γ_∞, is just (14e). Finally, (12b) and (12c) are simply (14c) and (14f). □

Theorem 3.2. *Problem* (14) *is well-posed.*

Proof. See Proof B.6. □

3.2 Basic ingredients of the coupling procedure

The coupling procedure hinges on a weak formulation in the interior domain Ω^- and a Dirichlet-to-Neumann map (DtN) associated with the classical Helmholtz equation (14b) in the exterior domain Ω^+.

3.2.1 Derivation of Dirichlet-to-Neumann maps

For $u \in H^1(\Omega^+ \cup \Omega^-)$, the jump and average of its Dirichlet traces across Γ_∞ are defined respectively as $[\gamma_0 u]_{\Gamma_\infty} := \gamma_0^+ u^+ - \gamma_0^- u^-$ and $\{\gamma_0 u\}_{\Gamma_\infty} := \frac{1}{2}\left(\gamma_0^+ u^+ + \gamma_0^- u^-\right)$. For $u \in H(\Delta, \Omega^+ \cup \Omega^-)$, the jump and average of its Neumann traces across Γ_∞ are defined respectively as $[\gamma_1 u]_{\Gamma_\infty} := \gamma_1^+ u^+ - \gamma_1^- u^-$ and $\{\gamma_1 u\}_{\Gamma_\infty} := \frac{1}{2}\left(\gamma_1^+ u^+ + \gamma_1^- u^-\right)$.

In what follows, Helmholtz equations, as well as corresponding boundary integral operators, are written for the transformed wave number $\hat{k}_\infty$. A function u defined over $\mathbb{R}^3$ is said to be a piecewise Helmholtz solution if $u|_{\Omega^+}$ and $u|_{\mathbb{R}^3\setminus\Omega^+}$ solve the classical Helmholtz equation (14b) respectively in Ω^+ and $\mathbb{R}^3\setminus\Omega^+$. A radiating piecewise Helmholtz solution is a piecewise Helmholtz solution that satisfies the Sommerfeld radiation condition (14f). For all $\lambda \in C^0(\Gamma_\infty)$, the single-layer potential is defined as $\mathcal{S}(\lambda)(\boldsymbol{x}) := \int_{\Gamma_\infty} E(\boldsymbol{y}-\boldsymbol{x})\lambda(\boldsymbol{y})ds(\boldsymbol{y})$, $\boldsymbol{x} \in \mathbb{R}^3\setminus\Gamma_\infty$, where $E(\boldsymbol{x}) := \frac{\exp(i\hat{k}_\infty|\boldsymbol{x}|)}{4\pi|\boldsymbol{x}|}$ is the fundamental solution of the classical Helmholtz equation (14b) with wave number $\hat{k}_\infty$ satisfying the Sommerfeld radiation condition (14f). For all $\mu \in C^0(\Gamma_\infty)$, the double-layer potential is defined as $\mathcal{D}(\mu)(\boldsymbol{x}) := \int_{\Gamma_\infty} \boldsymbol{\nabla_y} E(\boldsymbol{y}-\boldsymbol{x})\mu(\boldsymbol{y})ds(\boldsymbol{y})$, $\boldsymbol{x} \in \mathbb{R}^3\setminus\Gamma_\infty$. From [35, Theorem 3.1.16], these operators can be extended to bounded linear operators $\mathcal{S} : H^{-\frac{1}{2}}(\Gamma_\infty) \to H^1_{\text{loc}}(\mathbb{R}^3)$ and $\mathcal{D} : H^{\frac{1}{2}}(\Gamma_\infty) \to H^1_{\text{loc}}(\mathbb{R}^3\setminus\Gamma_\infty)$. Moreover, both map onto radiating piecewise Helmholtz solutions. Recalling [25, Theorem 3.1.1], a radiating piecewise Helmholtz solution u can be represented from its Dirichlet and Neumann jumps across Γ_∞ in the form

$$u = -\mathcal{S}([\gamma_1 u]_{\Gamma_\infty}) + \mathcal{D}([\gamma_0 u]_{\Gamma_\infty}) \quad \text{in } \Omega^+ \cup (\mathbb{R}^3\setminus\Omega^+). \tag{15}$$

The single-layer and double-layer potentials satisfy the following jump relations across Γ_∞ [25, Theorem 3.1.2]:

$$\begin{aligned}
&[\gamma_0(\mathcal{S}\lambda)]_{\Gamma_\infty} = 0, \qquad [\gamma_1(\mathcal{S}\lambda)]_{\Gamma_\infty} = -\lambda, \qquad \forall\lambda \in H^{-\frac{1}{2}}(\Gamma_\infty),\\
&[\gamma_0(\mathcal{D}\mu)]_{\Gamma_\infty} = \mu, \qquad [\gamma_1(\mathcal{D}\mu)]_{\Gamma_\infty} = 0, \qquad \forall\mu \in H^{\frac{1}{2}}(\Gamma_\infty),
\end{aligned} \tag{16}$$

with the operators

$$\begin{aligned}
&S : H^{-\frac{1}{2}}(\Gamma_\infty) \to H^{\frac{1}{2}}(\Gamma_\infty), && S\lambda := \gamma_0(\mathcal{S}\lambda),\\
&D : H^{\frac{1}{2}}(\Gamma_\infty) \to H^{\frac{1}{2}}(\Gamma_\infty), && D\mu := \{\gamma_0(\mathcal{D}\mu)\}_{\Gamma_\infty},\\
&\tilde{D} : H^{-\frac{1}{2}}(\Gamma_\infty) \to H^{-\frac{1}{2}}(\Gamma_\infty), && \tilde{D}\lambda := \{\gamma_1(\mathcal{S}\lambda)\}_{\Gamma_\infty},\\
&N : H^{\frac{1}{2}}(\Gamma_\infty) \to H^{-\frac{1}{2}}(\Gamma_\infty), && N\mu := -\gamma_1(\mathcal{D}\mu),
\end{aligned} \tag{17}$$

being respectively the single-layer, double-layer, transpose (or dual) of the double-layer, and hypersingular boundary integral operators. The Dirichlet and Neumann traces are well-defined, and the mapping properties can be found in [31, Theorem 7.1]. The following trace identities are directly derived from (16):

$$\begin{aligned}
&\gamma_0\mathcal{S} = S, && \gamma_1^\pm\mathcal{S} = \tilde{D} \mp \frac{1}{2}I,\\
&\gamma_0^\pm\mathcal{D} = D \pm \frac{1}{2}I, && \gamma_1\mathcal{D} = -N,
\end{aligned} \tag{18}$$

Moreover, if u is a radiating piecewise Helmholtz solution, taking the interior traces of (15) and using (18) leads to

$$\begin{pmatrix} \frac{1}{2}I - D & S \\ N & \frac{1}{2}I + \tilde{D} \end{pmatrix} \begin{pmatrix} [\gamma_0 u]_{\Gamma_\infty} \\ [\gamma_1 u]_{\Gamma_\infty} \end{pmatrix} = -\begin{pmatrix} \gamma_0^- u^- \\ \gamma_1^- u^- \end{pmatrix}. \tag{19}$$

Let now f solve (14) and let v be the function defined by $v|_{\Omega^+} := f_{\text{sc}}$ and $v|_{\mathbb{R}^3\setminus\Omega^+} := -f^-_{\text{inc}}$. The function v is a radiating piecewise Helmholtz solution (on Ω^+ this follows from (14b) and (14f), and

on $\mathbb{R}^3\backslash\Omega^+$ from (9)). Since f_{inc} is continuous across Γ_∞,

$$[\gamma_0 v]_{\Gamma_\infty} = \gamma_0^+ f_{\text{sc}} + \gamma_0^- f_{\text{inc}}^- = \gamma_0^+ f_{\text{sc}} + \gamma_0^+ f_{\text{inc}}^+ = \gamma_0^+ f^+. \tag{20}$$

Likewise, $[\gamma_1 v]_{\Gamma_\infty} = \gamma_1^+ f^+$. In what follows, we drop $\pm$ superscripts for the Dirichlet and Neumann traces of f and f_{inc} since the traces are continuous. Then, (19) applied to $u = v$ yields

$$\begin{pmatrix} \frac{1}{2}I - D & S \\ N & \frac{1}{2}I + \tilde{D} \end{pmatrix} \begin{pmatrix} \gamma_0 f \\ \gamma_1 f \end{pmatrix} = \begin{pmatrix} \gamma_0 f_{\text{inc}} \\ \gamma_1 f_{\text{inc}} \end{pmatrix}. \tag{21}$$

Various identities relating $\gamma_0 f$ and $\gamma_1 f$ can be derived from (21), and these identities can be used to define DtN maps. For example, using the first line of (21), $\gamma_1 f = DtN_0(\gamma_0 f) := S^{-1}\left(\gamma_0 f_{\text{inc}} + \left(D - \frac{1}{2}I\right)\gamma_0 f\right)$, where the question of the inversibility of S has to be addressed. Two other examples are detailed in Sections 3.3 and 3.4 below.

Remark 3.3. *The block operator defined on the left-hand side of* (21) *is not injective.*

3.2.2 Weak formulation in the interior domain Ω^-

Let $\Phi := f|_{\Omega^-}$ where f solves (14). Multiplying (14a) by a test function $\Phi^t \in H^1(\Omega^-)$ and using a Green formula yields

$$\mathcal{V}(\Phi, \Phi^t) - Q_\Gamma - \left(\gamma_1^- \Phi, \gamma_0^- \Phi^t\right)_{\Gamma_\infty} = 0, \tag{22}$$

with the sesquilinear form

$$\mathcal{V}(\Phi, \Phi^t) := \int_{\Omega^-} r\Xi\boldsymbol{\nabla}\overline{\Phi}\cdot\boldsymbol{\nabla}\Phi^t - \int_{\Omega^-} rk^2\beta\overline{\Phi}\Phi^t + i\int_{\Omega^-} rk\boldsymbol{V}\cdot\left(\overline{\Phi}\boldsymbol{\nabla}\Phi^t - \Phi^t\boldsymbol{\nabla}\overline{\Phi}\right) \tag{23}$$

and the boundary term $Q_\Gamma := \left(\gamma_{n,\Gamma}^- \left(irk\Phi\boldsymbol{V} + r\Xi\boldsymbol{\nabla}\Phi\right)^-, \gamma_{0,\Gamma}^-\Phi^t\right)_\Gamma$, where $\gamma_{0,\Gamma}^-$ denotes the one-sided Dirichlet trace on Γ from Ω^-. Owing to (14c), $Q_\Gamma = 0$. Hence, a weak formulation in the interior domain Ω^- is: Find $\Phi \in H^1(\Omega^-)$ such that $\forall \Phi^t \in H^1(\Omega^-)$,

$$\mathcal{V}(\Phi, \Phi^t) - \left(\gamma_1^- \Phi, \gamma_0^- \Phi^t\right)_{\Gamma_\infty} = 0. \tag{24}$$

Using the transmission conditions (14d)-(14e), $\gamma_0^-\Phi = \gamma_0 f$ and $\gamma_1^-\Phi = \gamma_1 f$, so that the coupling with the exterior problem can be written as $\gamma_1^-\Phi = DtN(\gamma_0^-\Phi)$. This yields the following coupled formulation: Find $\Phi \in H^1(\Omega^-)$ such that $\forall \Phi^t \in H^1(\Omega^-)$,

$$\mathcal{V}(\Phi, \Phi^t) - \left(DtN(\gamma_0^-\Phi), \gamma_0^-\Phi^t\right)_{\Gamma_\infty} = 0. \tag{25}$$

3.3 Unstable coupled formulation

To carry out the coupling, a first classical DtN map is considered. Since this DtN map is not well-defined at some frequencies, the resulting coupled formulation is not well-posed at these frequencies, and is therefore called unstable. From (21), recalling $\gamma_0^-\Phi = \gamma_0 f$ and $\gamma_1^-\Phi = \gamma_1 f$, there holds

$$\begin{pmatrix} \frac{1}{2}I - D & S \\ N & \frac{1}{2}I + \tilde{D} \end{pmatrix} \begin{pmatrix} \gamma_0^- \Phi \\ \gamma_1^- \Phi \end{pmatrix} = \begin{pmatrix} \gamma_0 f_{\text{inc}} \\ \gamma_1 f_{\text{inc}} \end{pmatrix}. \tag{26}$$

Using the first line of (26), $\gamma_1^-\Phi = S^{-1}\left(\left(D - \frac{1}{2}I\right)\left(\gamma_0^-\Phi\right) + \gamma_0 f_{\text{inc}}\right)$. At this point, the inverse of S is written formally. Conditions of inversibility are discussed below. From the second line of (26), $\gamma_1^-\Phi = -N(\gamma_0^-\Phi) + \left(\frac{1}{2}I - \tilde{D}\right)\left(\gamma_1^-\Phi\right) + \gamma_1 f_{\text{inc}}$. Injecting into the right-hand side of this relation the expression of $\gamma_1^-\Phi$ derived above yields the DtN affine map: $DtN_{\text{unstab}} : H^{\frac{1}{2}}(\Gamma_\infty) \to H^{-\frac{1}{2}}(\Gamma_\infty)$ such that

$$\gamma_1^-\Phi = DtN_{\text{unstab}}(\gamma_0^-\Phi) := -N(\gamma_0^-\Phi) + \left(\frac{1}{2}I - \tilde{D}\right)S^{-1}\left(\left(D - \frac{1}{2}I\right)(\gamma_0^-\Phi) + \gamma_0 f_{\text{inc}}\right) + \gamma_1 f_{\text{inc}}. \tag{27}$$

The operator inversion requires to introduce the auxiliary field $\lambda \in H^{-\frac{1}{2}}(\Gamma_\infty)$ such that

$$\left(D - \frac{1}{2}I\right)(\gamma_0^- \Phi) - S\lambda = -\gamma_0 f_{\text{inc}}, \tag{28}$$

yielding

$$DtN_{\text{unstab}}(\gamma_0^- \Phi) = -N(\gamma_0^- \Phi) + \left(\frac{1}{2}I - \tilde{D}\right)(\lambda) + \gamma_1 f_{\text{inc}}. \tag{29}$$

Injecting $DtN_{\text{unstab}}(\gamma_0^- \Phi)$ from (29) into the formulation (25) yields, using (28), the following coupled variational formulation: Find $(\Phi, \lambda) \in \mathcal{H}$ such that, $\forall \left(\Phi^t, \lambda^t\right) \in \mathcal{H}$,

$$\mathcal{V}(\Phi, \Phi^t) + \left(N(\gamma_0^- \Phi), \gamma_0^- \Phi^t\right)_{\Gamma_\infty} + \left(\left(\tilde{D} - \frac{1}{2}I\right)(\lambda), \gamma_0^- \Phi^t\right)_{\Gamma_\infty} = \left(\gamma_1 f_{\text{inc}}, \gamma_0^- \Phi^t\right)_{\Gamma_\infty}, \tag{30a}$$

$$\left(\lambda^t, \left(D - \frac{1}{2}I\right)(\gamma_0^- \Phi)\right)_{\Gamma_\infty} - \left(\lambda^t, S(\lambda)\right)_{\Gamma_\infty} = -\left(\lambda^t, \gamma_0 f_{\text{inc}}\right)_{\Gamma_\infty}, \tag{30b}$$

with product space $\mathcal{H} := H^1\left(\Omega^-\right) \times H^{-\frac{1}{2}}\left(\Gamma_\infty\right)$ and inner product $\left(\left(\Phi, \lambda\right), \left(\Phi^t, \lambda^t\right)\right)_{\mathcal{H}} := \left(\Phi, \Phi^t\right)_{H^1(\Omega^-)} + \left(\lambda, \lambda^t\right)_{H^{-\frac{1}{2}}(\Gamma_\infty)}$. The formulation (30) is called unstable since it admits infinitely many solutions at some frequencies of the source, leading to incorrect numerical results.

Remark 3.4. *The DtN_{unstab} affine map was proposed by Costabel to obtain a symmetric coupling in the case of self-adjoint operators [10]. The DtN_{unstab} map can be well-defined for certain operators: for instance, for transmission problems for the Laplace equation, this map leads to a well-defined symmetric system. In the system* (30)*, the only non-symmetric contribution results from the vector $\boldsymbol{V}$ in the sesquilinear form $\mathcal{V}$. The system becomes symmetric when the flow is uniform everywhere. However, since D and $\tilde{D}$ are dual but not adjoint operators, there is no Hermitian symmetry.*

Proposition 3.5. *If f solves* (14)*, then $(f^-, \gamma_1 f)$ solves* (30)*. Conversely, if (Φ, λ) solves* (30)*, then $\mathcal{R}(\Phi, \lambda)$ solves* (14)*, where $\mathcal{R} : \mathcal{H} \to H^1_{\text{loc}}(\Omega \backslash \Gamma_\infty)$ is such that $\mathcal{R}(\Phi, \lambda)|_{\Omega^-} := \Phi$ and $\mathcal{R}(\Phi, \lambda)|_{\Omega^+} := (-\mathcal{S}(\lambda) + \mathcal{D}(\gamma_0^- \Phi) + f_{\text{inc}})|_{\Omega^+}$.*

Proof. See Proof B.7. ☐

The main difficulty with the unstable coupled formulation (30) stems from the fact that $\ker(S)$ depends on whether $-\hat{k}_\infty^2$ belongs to the set Λ of Dirichlet eigenvalues for the Laplacian on the bounded domain $\mathbb{R}^3 \backslash \Omega^+$. Specifically, $\ker(S) = \{0\}$ if $-\hat{k}_\infty^2 \notin \Lambda$, while $\ker(S)$ contains nontrivial elements if $-\hat{k}_\infty^2 \in \Lambda$.

Proposition 3.6. *If f solves* (14)*, then for all $\lambda^* \in \ker(S)$, $(f^-, \gamma_1 f + \lambda^*)$ solves* (30)*.*

Proof. This is a direct consequence of $\ker(S) = \ker(\tilde{D} - \frac{1}{2}I)$. ☐

Theorem 3.7. *If $-\hat{k}_\infty^2 \notin \Lambda$, then problem* (30) *is well-posed. If $-\hat{k}_\infty^2 \in \Lambda$, then* (30) *admits infinitely many solutions of the form $(f^-, \gamma_1 f + \lambda^*)$, where f is the solution to* (14) *and λ^* is any element in* $\ker(S)$.

Proof. See Proof B.8. ☐

Remark 3.8. *Let $-\hat{k}_\infty^2 \in \Lambda$. Owing to Proposition 3.5, for any couple (Φ, λ) solving* (30)*, $\mathcal{R}(\Phi, \lambda)$ solves* (14)*. However, even if our goal is to solve* (14)*, we will see in Section 5 that the numerical procedure to approximate* (30) *fails to the point that $\mathcal{R}(\Phi, \lambda)$ is dominated by numerical errors.*

3.4 Stable coupled formulation

The idea of considering a linear combination of S and $\frac{1}{2}I + \tilde{D}$ to derive well-posed boundary integral equations was independently proposed in 1965 by Brakhage and Werner [5], Leis [27] and Panich [33]. This is the so-called Combined Field Integral Equation (CFIE). However, S and D map $H^{-\frac{1}{2}}(\Gamma_\infty)$ into different spaces ($H^{\frac{1}{2}}(\Gamma_\infty)$ and $H^{-\frac{1}{2}}(\Gamma_\infty)$ respectively). This inconsistency in the functional setting can be solved by considering a regularizing compact operator from $H^{-\frac{1}{2}}(\Gamma_\infty)$ into $H^{\frac{1}{2}}(\Gamma_\infty)$, as observed by Buffa and Hiptmair [7]. We briefly recall the approach of [7] and apply it to the present setting. Let $\boldsymbol{\nabla}_{\Gamma_\infty}$ denote the surfacic gradient on Γ_∞. Consider the following Hermitian sesquilinear form: For all $p, q \in H^1(\Gamma_\infty)$,

$$\delta_{\Gamma_\infty}(p,q) := (\boldsymbol{\nabla}_{\Gamma_\infty} p, \boldsymbol{\nabla}_{\Gamma_\infty} q)_{\Gamma_\infty} + (p,q)_{\Gamma_\infty}, \tag{31}$$

and the regularizing operator $M : H^{-1}(\Gamma_\infty) \to H^1(\Gamma_\infty)$ defined through the following implicit relation: For all $p \in H^1(\Gamma_\infty)$,

$$\delta_{\Gamma_\infty}(Mp, q) = (p,q)_{\Gamma_\infty}, \quad \forall q \in H^1(\Gamma_\infty). \tag{32}$$

It is readily seen that $M = (-\Delta_{\Gamma_\infty} + I)^{-1}$, where Δ_{Γ_∞} is the Laplace–Beltrami operator on Γ_∞.

Many choices of DtN maps based on CFIE strategies with the regularizing operator M lead to well-posed systems whatever the value of $\hat{k}_\infty$. The present choice hinges on the inversion of the operator $S + i\eta M\left(\frac{1}{2}I + \tilde{D}\right)$ mapping $H^{-\frac{1}{2}}(\Gamma_\infty)$ into $H^{\frac{1}{2}}(\Gamma_\infty)$ since, from [7, Lemma 4.1], this operator is bijective as long as the coupling parameter η is such that $\mathrm{Re}(\eta) \neq 0$. To do so, the first line of (26) and the application of M to the second line of (26) are used to obtain

$$\begin{pmatrix} \left(\frac{1}{2}I - D\right) + i\eta MN & S + i\eta M\left(\frac{1}{2}I + \tilde{D}\right) \\ N & \frac{1}{2}I + \tilde{D} \end{pmatrix} \begin{pmatrix} \gamma_0^- \Phi \\ \gamma_1^- \Phi \end{pmatrix} = \begin{pmatrix} \gamma_0 f_{\mathrm{inc}} + i\eta M \gamma_1 f_{\mathrm{inc}} \\ \gamma_1 f_{\mathrm{inc}} \end{pmatrix}. \tag{33}$$

Then, using both equations in (33) in the same fashion as in Section 3.3 leads to $DtN_{\mathrm{stab}} : H^{\frac{1}{2}}(\Gamma_\infty) \to H^{-\frac{1}{2}}(\Gamma_\infty)$ such that

$$\begin{aligned} \gamma_1^- \Phi = & DtN_{\mathrm{stab}}(\gamma_0^- \Phi) := -N(\gamma_0^- \Phi) + \left(\frac{1}{2}I - \tilde{D}\right)\left[S + i\eta M\left(\frac{1}{2}I + \tilde{D}\right)\right]^{-1} \\ & \left(-\left[\left(\frac{1}{2}I - D\right) + i\eta MN\right](\gamma_0^- \Phi) + \gamma_0 f_{\mathrm{inc}} + i\eta M \gamma_1 f_{\mathrm{inc}}\right) + \gamma_1 f_{\mathrm{inc}}. \end{aligned} \tag{34}$$

The operator inversion requires to introduce the auxiliary field $\lambda \in H^{-\frac{1}{2}}(\Gamma_\infty)$ such that

$$\left[S + i\eta M\left(\frac{1}{2}I + \tilde{D}\right)\right](\lambda) + \left[\left(\frac{1}{2}I - D\right) + i\eta MN\right](\gamma_0^- \Phi) = \gamma_0 f_{\mathrm{inc}} + i\eta M(\gamma_1 f_{\mathrm{inc}}), \tag{35}$$

so that

$$DtN_{\mathrm{stab}}(\gamma_0^- \Phi) = -N(\gamma_0^- \Phi) + \left(\frac{1}{2}I - \tilde{D}\right)(\lambda) + \gamma_1 f_{\mathrm{inc}}. \tag{36}$$

The evaluation of M involving an operator inversion as well, it requires to introduce another auxiliary field $p \in H^1(\Gamma_\infty)$ such that, for all $q \in H^1(\Gamma_\infty)$,

$$\delta_{\Gamma_\infty}(p,q) = \left(N(\gamma_0^- \Phi), q\right)_{\Gamma_\infty} + \left(\left(\frac{1}{2}I + \tilde{D}\right)(\lambda), q\right)_{\Gamma_\infty} - (\gamma_1 f_{\mathrm{inc}}, q)_{\Gamma_\infty}, \tag{37}$$

so that equation (35) can be rewritten

$$S(\lambda) + \left(\frac{1}{2}I - D\right)(\gamma_0^- \Phi) + i\eta p = \gamma_0 f_{\mathrm{inc}}. \tag{38}$$

Injecting $DtN_{\mathrm{stab}}(\gamma_0^- \Phi)$ from (36) into the formulation (25) yields, using (38) and (37), the following stable coupled variational formulation: Find $(\Phi, \lambda, p) \in \mathbb{H}$ such that $\forall \left(\Phi^t, \lambda^t, p^t\right) \in \mathbb{H}$,

$$\mathcal{V}(\Phi, \Phi^t) + \left(N(\gamma_0^- \Phi), \gamma_0^- \Phi^t\right)_{\Gamma_\infty} + \left(\left(\tilde{D} - \frac{1}{2}I\right)(\lambda), \gamma_0^- \Phi^t\right)_{\Gamma_\infty} = \left(\gamma_1 f_{\mathrm{inc}}, \gamma_0^- \Phi^t\right)_{\Gamma_\infty}, \tag{39a}$$

$$\left(\lambda^t, \left(D - \frac{1}{2}I\right)(\gamma_0^- \Phi)\right)_{\Gamma_\infty} - \left(\lambda^t, S(\lambda)\right)_{\Gamma_\infty} - i\eta\left(\lambda^t, p\right)_{\Gamma_\infty} = -\left(\lambda^t, \gamma_0 f_{\mathrm{inc}}\right)_{\Gamma_\infty}, \tag{39b}$$

$$\left(N(\gamma_0^- \Phi), p^t\right)_{\Gamma_\infty} + \left(\left(\tilde{D} + \frac{1}{2}I\right)(\lambda), p^t\right)_{\Gamma_\infty} - \delta_{\Gamma_\infty}(p, p^t) = \left(\gamma_1 f_{\mathrm{inc}}, p^t\right)_{\Gamma_\infty}, \tag{39c}$$

with product space $\mathbb{H} := H^1(\Omega^-) \times H^{-\frac{1}{2}}(\Gamma_\infty) \times H^1(\Gamma_\infty)$ and inner product $\left((\Phi, \lambda, p), \left(\Phi^t, \lambda^t, p^t\right)\right)_{\mathbb{H}} := \left(\Phi, \Phi^t\right)_{H^1(\Omega^-)} + \left(\lambda, \lambda^t\right)_{H^{-\frac{1}{2}}(\Gamma_\infty)} + \left(p, p^t\right)_{H^1(\Gamma_\infty)}$.

Proposition 3.9. *If f solves (14), then $(f^-, \gamma_1 f, 0)$ solves (39). Conversely, if (Φ, λ, p) solves (39), then $\mathcal{R}(\Phi, \lambda)$ solves (14) and $p = 0$, where $\mathcal{R}$ is defined in Proposition 3.5.*

Proof. See Proof B.3. □

Theorem 3.10. *Problem (39) is well-posed at all frequencies.*

Proof. See Proof B.5. □

Remark 3.11. *Hiptmair and Meury [22] derived abstract trace transformation operators and generalized Calderón projectors for the Helmholtz transmission problem. By construction, integral operators written using these projectors enjoy the uniqueness property whatever the value of $\hat{k}_\infty$. The map DtN_{stab} corresponds to a particular choice of the trace transformation operator in the general setting of [22, Section 9]. Hence, Theorem 3.10 is an extension of [22, Theorem 7.3] to the non-zero flow case, for a particular choice of the trace transformation operator.*

4 Finite-dimensional approximation

The coupled formulations (30) and (39) are approximated by finite element and boundary element methods. The underlying results are well-known from both theories and can be directly applied to the present setting.

4.1 Discrete finite element spaces

Let $\mathcal{M}$ be a shape-regular tetrahedral mesh of Ω^-. The mesh $\mathcal{F}_\infty$ of Γ_∞ is composed of the boundary faces of $\mathcal{M}$. Let $h_\mathcal{M} > 0$ denote the mesh size, $V^1_\mathcal{M}$ the space of continuous piecewise affine polynomials on $\mathcal{M}$, $S^0_\mathcal{M}$ the space of piecewise constant polynomials on $\mathcal{F}_\infty$, and $S^1_\mathcal{M}$ the space of continuous piecewise affine polynomials on $\mathcal{F}_\infty$. Let $\mathcal{H}_\mathcal{M} := V^1_\mathcal{M} \times S^0_\mathcal{M}$, and $\mathbb{H}_\mathcal{M} := V^1_\mathcal{M} \times S^0_\mathcal{M} \times S^1_\mathcal{M}$. The discretization of (30) reads: Find $(\Phi_\mathcal{M}, \lambda_\mathcal{M}) \in \mathcal{H}_\mathcal{M}$ such that, $\forall \left(\Phi^t_\mathcal{M}, \lambda^t_\mathcal{M}\right) \in \mathcal{H}_\mathcal{M}$,

$$a^{\mathrm{unstab}}\left((\Phi_\mathcal{M}, \lambda_\mathcal{M}), \left(\Phi^t_\mathcal{M}, \lambda^t_\mathcal{M}\right)\right) = b^{\mathrm{unstab}}\left(\Phi^t_\mathcal{M}, \lambda^t_\mathcal{M}\right), \tag{40}$$

with a^{unstab} and b^{unstab} readily deduced from (30), while the discretization of (39) reads: Find $(\Phi_\mathcal{M}, \lambda_\mathcal{M}, p_\mathcal{M}) \in \mathbb{H}_\mathcal{M}$ such that, $\forall \left(\Phi^t_\mathcal{M}, \lambda^t_\mathcal{M}, p^t_\mathcal{M}\right) \in \mathbb{H}_\mathcal{M}$,

$$a^{\mathrm{stab}}\left((\Phi_\mathcal{M}, \lambda_\mathcal{M}, p_\mathcal{M}), \left(\Phi^t_\mathcal{M}, \lambda^t_\mathcal{M}, p^t_\mathcal{M}\right)\right) = b^{\mathrm{stab}}\left(\Phi^t_\mathcal{M}, \lambda^t_\mathcal{M}, p^t_\mathcal{M}\right), \tag{41}$$

with a^{stab} and b^{stab} readily deduced from (39). Since $\mathcal{H}_\mathcal{M} \subset \mathcal{H}$ and $\mathbb{H}_\mathcal{M} \subset \mathbb{H}$, both approximations are conforming.

In what follows, $A \lesssim B$ denotes the inequality $A \leq cB$ with positive constant c independent of the mesh size and of the discrete and exact solutions. The following classical approximation properties are available (see [6, 16, 35]):

$$\begin{aligned}
\inf_{\Phi_{\mathcal{M}}\in V^1_{\mathcal{M}}} \|\Phi - \Phi_{\mathcal{M}}\|_{H^1(\Omega^-)} &\lesssim h_{\mathcal{M}} \|\Phi\|_{H^2(\Omega^-)}\,, \\
\inf_{\lambda_{\mathcal{M}}\in S^0_{\mathcal{M}}} \|\lambda - \lambda_{\mathcal{M}}\|_{H^{-\frac{1}{2}}(\Gamma_\infty)} &\lesssim h_{\mathcal{M}} \|\lambda\|_{H^{\frac{1}{2}}(\Gamma_\infty)}\,, \\
\inf_{p_{\mathcal{M}}\in S^1_{\mathcal{M}}} \|p - p_{\mathcal{M}}\|_{H^1(\Gamma_\infty)} &\lesssim h_{\mathcal{M}} \|p\|_{H^2(\Gamma_\infty)}\,.
\end{aligned} \tag{42}$$

Hence, the following approximation properties hold: $\forall(\Phi,\lambda) \in H^2(\Omega^-)\times H^{\frac{1}{2}}(\Gamma_\infty)$,

$$\inf_{(\Phi_{\mathcal{M}},\lambda_{\mathcal{M}})\in\mathcal{H}_{\mathcal{M}}} \|(\Phi,\lambda) - (\Phi_{\mathcal{M}},\lambda_{\mathcal{M}})\|_{\mathcal{H}} \lesssim h_{\mathcal{M}}\left(\|\Phi\|_{H^2(\Omega^-)} + \|\lambda\|_{H^{\frac{1}{2}}(\Gamma_\infty)}\right), \tag{43}$$

and $\forall(\Phi,\lambda,p) \in H^2(\Omega^-)\times H^{\frac{1}{2}}(\Gamma_\infty)\times H^2(\Gamma_\infty)$,

$$\inf_{(\Phi_{\mathcal{M}},\lambda_{\mathcal{M}},p_{\mathcal{M}})\in\mathbb{H}_{\mathcal{M}}} \|(\Phi,\lambda,p) - (\Phi_{\mathcal{M}},\lambda_{\mathcal{M}},p_{\mathcal{M}})\|_{\mathbb{H}} \lesssim h_{\mathcal{M}}\left(\|\Phi\|_{H^2(\Omega^-)} + \|\lambda\|_{H^{\frac{1}{2}}(\Gamma_\infty)} + \|p\|_{H^2(\Gamma_\infty)}\right). \tag{44}$$

Remark 4.1. *Taking a polynomial approximation with one order less for $H^{-\frac{1}{2}}(\Gamma_\infty)$ than for $H^1(\Omega^-)$ and $H^1(\Gamma_\infty)$ enables all the approximations to be at the same order in $h_{\mathcal{M}}$.*

4.2 Discretization of the coupled formulations

Let $(\theta_i)_{1\leq i\leq p}$ and $(\psi_i)_{1\leq i\leq q}$ denote finite element bases for $V^1_{\mathcal{M}}$ and $S^0_{\mathcal{M}}$ respectively. The decompositions of $\Phi_{\mathcal{M}} \in V^1_{\mathcal{M}}$ and $\lambda_{\mathcal{M}} \in S^0_{\mathcal{M}}$ on these bases are written in the form $\Phi_{\mathcal{M}} = \sum_{i=1}^p \Phi_{\mathcal{M}i}\theta_i$ and $\lambda_{\mathcal{M}} = \sum_{i=1}^q \lambda_{\mathcal{M}i}\psi_i$. Let

$$u^{\text{unstab}}_{\mathcal{M}} = \begin{pmatrix} (\Phi_{\mathcal{M}i})_{\ 1\leq i\leq p} \\ (\lambda_{\mathcal{M}i})_{\ 1\leq i\leq q}\end{pmatrix}, \qquad B^{\text{unstab}} = \begin{pmatrix} \left(\gamma_1 f_{\text{inc}}, \gamma_0^-\theta_i\right)_{\Gamma_\infty\ 1\leq i\leq p} \\ -\left(\psi_i, \gamma_0 f_{\text{inc}}\right)_{\Gamma_\infty\ 1\leq i\leq q}\end{pmatrix}, \tag{45}$$

$$A^{\text{unstab}} = \left(\begin{array}{c|c} \mathcal{V}(\theta_j,\theta_i) + \left(N(\gamma_0^-\theta_j),\gamma_0^-\theta_i\right)_{\Gamma_\infty} & \left(\left(\tilde{D}-\frac{1}{2}I\right)(\psi_j),\gamma_0^-\theta_i\right)_{\Gamma_\infty} \\ \hline \left(\psi_i,\left(D-\frac{1}{2}I\right)(\gamma_0^-\theta_j)\right)_{\Gamma_\infty} & -(\psi_i,S(\psi_j))_{\Gamma_\infty}\end{array}\right), \tag{46}$$

where in A^{unstab} the index i refers to the lines and the index j to the columns. The linear system resulting from (40) is

$$A^{\text{unstab}}u^{\text{unstab}}_{\mathcal{M}} = B^{\text{unstab}}. \tag{47}$$

Let $(\xi_i)_{1\leq i\leq r}$ denote a finite element basis for $S^1_{\mathcal{M}}$. The decomposition of $p_{\mathcal{M}} \in S^1_{\mathcal{M}}$ on this basis is written in the form $p_{\mathcal{M}} = \sum_{i=1}^r p_{\mathcal{M}i}\xi_i$. Let

$$u^{\text{stab}}_{\mathcal{M}} = \begin{pmatrix} (\Phi_{\mathcal{M}i})_{\ 1\leq i\leq p} \\ (\lambda_{\mathcal{M}i})_{\ 1\leq i\leq q} \\ (p_{\mathcal{M}i})_{\ 1\leq i\leq r}\end{pmatrix}, \qquad B^{\text{stab}} = \begin{pmatrix} \left(\gamma_1 f_{\text{inc}}, \gamma_0^-\theta_i\right)_{\Gamma_\infty\ 1\leq i\leq p} \\ -\left(\psi_i, \gamma_0 f_{\text{inc}}\right)_{\Gamma_\infty\ 1\leq i\leq q} \\ \left(\gamma_1 f_{\text{inc}}, \xi_i\right)_{\Gamma_\infty\ 1\leq i\leq r}\end{pmatrix}, \tag{48}$$

$$A^{\text{stab}} = \left(\begin{array}{c|c|c} \mathcal{V}(\theta_j,\theta_i) + \left(N(\gamma_0^-\theta_j),\gamma_0^-\theta_i\right)_{\Gamma_\infty} & \left(\left(\tilde{D}-\frac{1}{2}I\right)(\psi_j),\gamma_0^-\theta_i\right)_{\Gamma_\infty} & 0 \\ \hline \left(\psi_i,\left(D-\frac{1}{2}I\right)(\gamma_0^-\theta_j)\right)_{\Gamma_\infty} & -(\psi_i,S(\psi_j))_{\Gamma_\infty} & -i\eta(\psi_i,\xi_j)_{\Gamma_\infty} \\ \hline \left(N(\gamma_0^-\theta_j),\xi_i\right)_{\Gamma_\infty} & \left(\left(\tilde{D}-\frac{1}{2}I\right)(\psi_j),\xi_i\right)_{\Gamma_\infty} & -\delta_{\Gamma_\infty}(\xi_j,\xi_i)_{\Gamma_\infty}\end{array}\right), \tag{49}$$

with the same convention on the indices i and j of A^{stab}. The linear system resulting from (41) is

$$A^{\text{stab}}u^{\text{stab}}_{\mathcal{M}} = B^{\text{stab}}. \tag{50}$$

4.3 Inf-sup stability of the discretized formulations

From the Fredholm setting and the approximation properties (43) and (44), the following discrete inf-sup conditions can be derived following [24, Theorem 14].

Proposition 4.2. *If $-\hat{k}_\infty^2 \notin \Lambda$ and $h_\mathcal{M}$ is small enough, there holds, for all $(\Phi_\mathcal{M}, \lambda_\mathcal{M}) \in \mathcal{H}_\mathcal{M}$,*

$$\sup_{(0,0)\neq\left(\Phi^t_\mathcal{M},\lambda^t_\mathcal{M}\right)\in\mathcal{H}_\mathcal{M}} \frac{\left|a^{\text{unstab}}\left((\Phi_\mathcal{M},\lambda_\mathcal{M}),\left(\Phi^t_\mathcal{M},\lambda^t_\mathcal{M}\right)\right)\right|}{\left\|\left(\Phi^t_\mathcal{M},\lambda^t_\mathcal{M}\right)\right\|_\mathcal{H}} \gtrsim \|(\Phi_\mathcal{M},\lambda_\mathcal{M})\|_\mathcal{H}. \tag{51}$$

At all frequencies and if $h_\mathcal{M}$ is small enough, there holds, for all $(\Phi_\mathcal{M}, \lambda_\mathcal{M}, p_\mathcal{M}) \in \mathbb{H}_\mathcal{M}$,

$$\sup_{(0,0,0)\neq\left(\Phi^t_\mathcal{M},\lambda^t_\mathcal{M},p^t_\mathcal{M}\right)\in\mathbb{H}_\mathcal{M}} \frac{\left|a^{\text{stab}}\left((\Phi_\mathcal{M},\lambda_\mathcal{M},p_\mathcal{M}),\left(\Phi^t_\mathcal{M},\lambda^t_\mathcal{M},p^t_\mathcal{M}\right)\right)\right|}{\left\|\left(\Phi^t_\mathcal{M},\lambda^t_\mathcal{M},p^t_\mathcal{M}\right)\right\|_\mathbb{H}} \gtrsim \|(\Phi_\mathcal{M},\lambda_\mathcal{M},p_\mathcal{M})\|_\mathbb{H}. \tag{52}$$

4.4 Convergence

From the inf-sup stability of the discrete problems, the following error estimates easily follow from [24, Theorem 13].

Proposition 4.3. *If $-\hat{k}_\infty^2 \notin \Lambda$ and $h_\mathcal{M}$ is small enough, the discrete problem* (40) *has a unique solution $(\Phi_\mathcal{M}, \lambda_\mathcal{M}) \in \mathcal{H}_\mathcal{M}$, and the following optimal error estimate holds:*

$$\|\,(\Phi,\lambda)-(\Phi_\mathcal{M},\lambda_\mathcal{M})\,\|_\mathcal{H} \lesssim \inf_{\left(\Phi^t_\mathcal{M},\lambda^t_\mathcal{M}\right)\in\mathcal{H}_\mathcal{M}} \|\,(\Phi,\lambda)-\left(\Phi^t_\mathcal{M},\lambda^t_\mathcal{M}\right)\|_\mathcal{H}, \tag{53}$$

where (Φ, λ) is the unique solution of (30). *At all frequencies and if $h_\mathcal{M}$ is small enough, the discrete problem* (41) *has a unique solution $(\Phi_\mathcal{M}, \lambda_\mathcal{M}, p_\mathcal{M}) \in \mathbb{H}_\mathcal{M}$, and the following optimal error estimate holds:*

$$\|\,(\Phi,\lambda,p)-(\Phi_\mathcal{M},\lambda_\mathcal{M},p_\mathcal{M})\,\|_\mathbb{H} \lesssim \inf_{\left(\Phi^t_\mathcal{M},\lambda^t_\mathcal{M},p^t_\mathcal{M}\right)\in\mathbb{H}_\mathcal{M}} \|\,(\Phi,\lambda,p)-\left(\Phi^t_\mathcal{M},\lambda^t_\mathcal{M},p^t_\mathcal{M}\right)\|_\mathbb{H}, \tag{54}$$

where (Φ, λ, p) is the unique solution of (39).

Remark 4.4. *The constant in* (53) *depends on $\hat{k}_\infty$, and its value explodes as $-\hat{k}_\infty^2$ tends to an element of Λ. The constant in* (54) *depends on $\hat{k}_\infty$ as well, but remains bounded on any bounded set of frequencies.*

5 Numerical results

The purpose of this section is the comparison between the unstable formulation (30) and the stable formulation (39) with the coupling parameter $\eta = 1$. Both formulations have been implemented in the EADS in-house boundary element software called ACTIPOLE [12, 13]. This software can treat general three-dimensional geometries. The iterative solver is a block generalized conjugate residual method [32, 26] based on a generalized minimal residual method [34], suitable for non-symmetric systems. A sparse approximate inverse preconditioner [8, 9] is used.

Consider an ellipsoid with major axis directed along the z-axis. This object is included inside a larger ball. The external border of the ball after discretization is the surface Γ_∞. A potential flow is computed around the ellipsoid and inside the ball, such that the flow is uniform outside the ball, of Mach number 0.3 and directed along the z-axis. An acoustic monopole source lies upstream of the ball, on the z-axis as well. Four different meshes are considered, see Table 1. Mesh 1 is such that the mean edge is ten times smaller than the wavelength at rest for a frequency of 1500 Hz. From Table 1, for fine meshes, the number of basis functions used to discretize the unknown p for the variational formulation (41) takes a smaller part in the total number of basis functions than for coarse meshes. Therefore, the relative complexity added to (30) by the third equation of (39) decreases with the total number of unknowns, which is an interesting property when it comes to industrial test cases. Figure 2 displays Mesh 1 and the rescaled velocity $\boldsymbol{M}_0$ of the potential flow.

In what follows, a frequency $\mathtt{f}$ is called resonant if $-\hat{k}_\infty^2 = -\frac{4\pi^2\mathtt{f}^2}{\gamma_\infty^2} \in \Lambda$, where Λ is the set of Dirichlet eigenvalues for the Laplacian on $\mathbb{R}^3\backslash\Omega^+$. The set Λ depends on the geometric shape of the coupling surface Γ_∞, which slightly changes after each discretization.

	Mesh 1	Mesh 2	Mesh 3	Mesh 4
number of volumic dofs Φ	1796	687	194	79
number of surfacic $\mathbb{P}_0$ dofs λ	808	510	270	148
number of surfacic $\mathbb{P}_1$ dofs p	406	257	137	76
proportion of dofs p in the total number of dofs	11.9%	15.0%	18.6%	20.0%
smallest edge (mm)	7.09	8.78	15.71	19.18
mean edge (mm)	22.64	32.20	49.78	66.46
largest edge (mm)	56.87	70.62	103.59	112.71

Table 1: Characteristics of the four considered meshes.

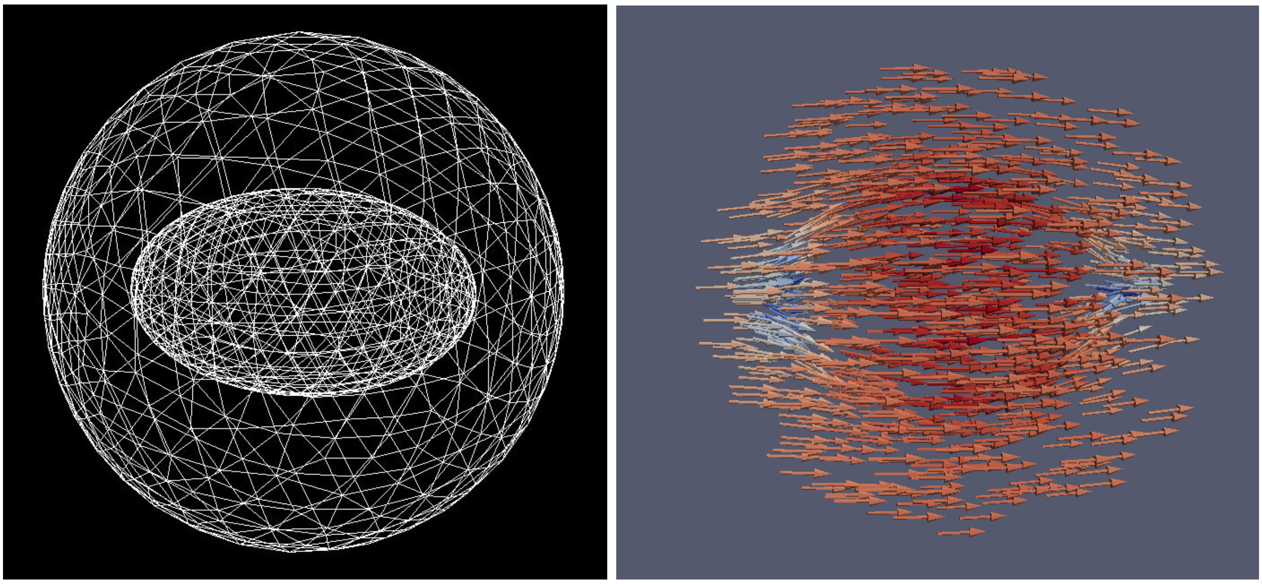

Figure 2: Left: representation of Mesh 1, Right: potential flow around the ellipsoid.

5.1 Comparison of pressure fields

As seen in Theorem 3.7, the unstable formulation (30) is not well-posed at resonant frequencies. First, a prospective study to identify a resonant frequency for each of the four meshes is carried out by monitoring the condition number of the matrices produced by the discretized version of the unstable formulation (30). A resonant frequency for Mesh 1, Mesh 2, Mesh 3, and Mesh 4 is identified around 1509.849 Hz, 1513.431 Hz, 1521.015 Hz, and 1535.704 Hz respectively.

The convergence of the iterative solver is monitored by requiring that the Euclidian norm of the relative residual is smaller than 10^{-6}. Additional tests indicate that the discretized solution to the stable formulation does not change much below this value of the relative residual. For Mesh 1, away from a resonance, say at 1500 Hz, the scattered pressure fields computed with the unstable and stable formulations are very similar. This holds as well for the total pressure fields, see Figure 3. At the resonant frequency 1509.849 Hz, the unstable formulation (30) yields pressure maps quite different from the ones at 1500 Hz, whereas the stable formulation (39) yields pressure maps very similar to the ones at 1500 Hz, see Figure 4. From Proposition 3.5, at a resonant frequency, the solutions to (30) that differ from the solution to (39) should not affect the scattered pressure field in the exterior domain. Actually, the distortion of the scattered field with the unstable formulation (30) is the result of the significant magnification of discretization and numerical errors by the ill-conditioning of the linear system approximating (30).

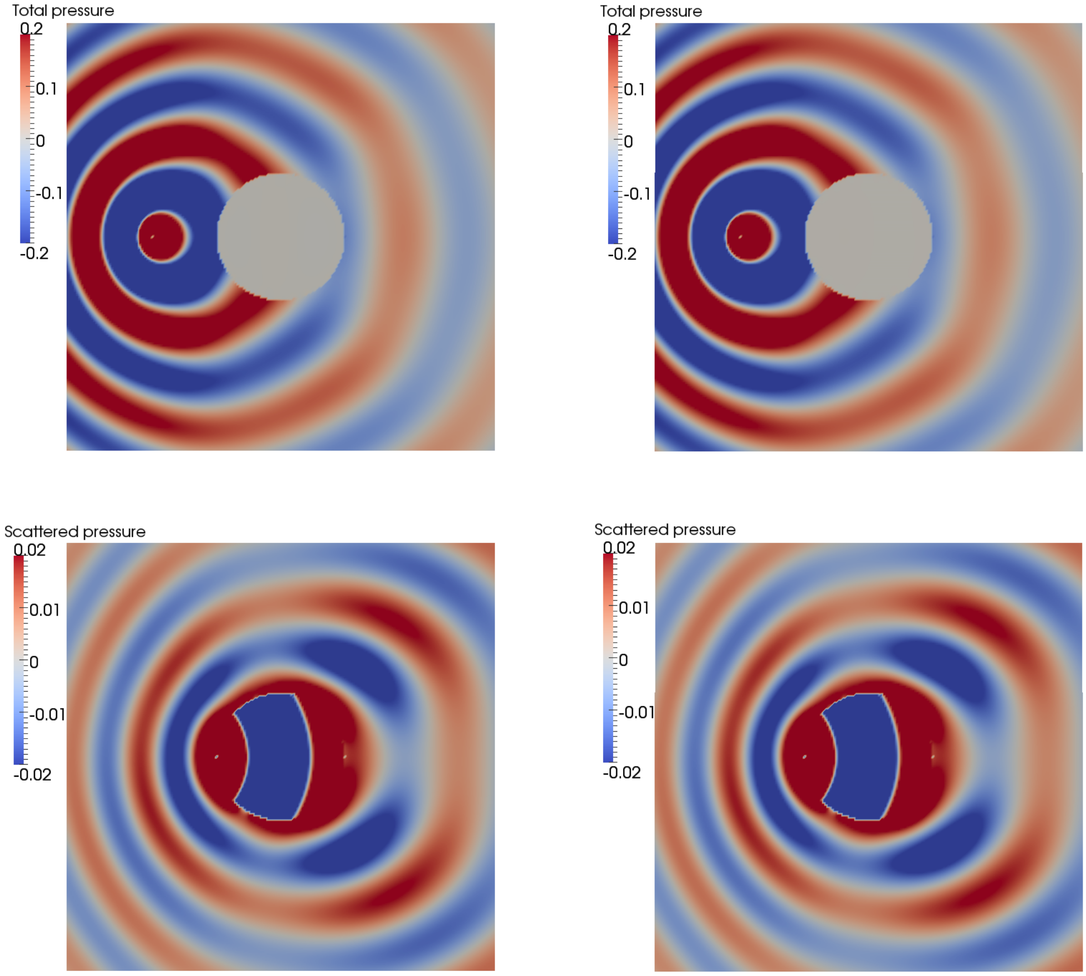

Figure 3: Mesh 1, 1500 Hz. Top : real part of the total pressure; left: unstable formulation (30), right: stable formulation (39). Bottom : real part of the scattered pressure; left: unstable formulation (30), right: stable formulation (39). At this non-resonant frequency, both formulations yield similar results.

5.2 Auxiliary variable p

In Figure 5, the left plot indicates that with Mesh 1, the magnitude of p is around 0.5% of the scattered pressure. The right plot shows the behaviour of the magnitude of p with respect to the stopping criterion of the iterative solver for the four meshes. The finer the mesh, the smaller the auxiliary variable p, which is consistent with the fact that the p-component of the solution to (39) vanishes (see Proposition 3.9).

5.3 Comparison of condition numbers

Figure 6 presents the condition numbers of the matrices resulting from the formulations (30) and (39) with respect to the frequency. In the left plot, the curves are centered at the resonant frequencies. The finer the mesh, the higher the condition number explodes. The width of the peak at the resonance does not appear to depend on the mesh. In the right plot, a larger bandwidth is considered with Mesh 2. Owing to the frequency sampling (every 5 Hz), some resonances may be missed and the local maxima may not be accurately reached (in particular, from the left plot, the local maximum of 7.2 for $\log(\mathrm{cond}(M))$ at 1513.431 Hz is very underestimated). The stable formulation (39) produces somewhat larger condition numbers for the large majority of the frequencies, but, unlike the unstable formulation (30), it presents no resonance. Moreover, from the Weyl formula, the number of resonant frequencies smaller than $\mathtt{f}$ increases as $\mathtt{f}^{\frac{3}{2}}$, making the need for a stable formulation even more important for

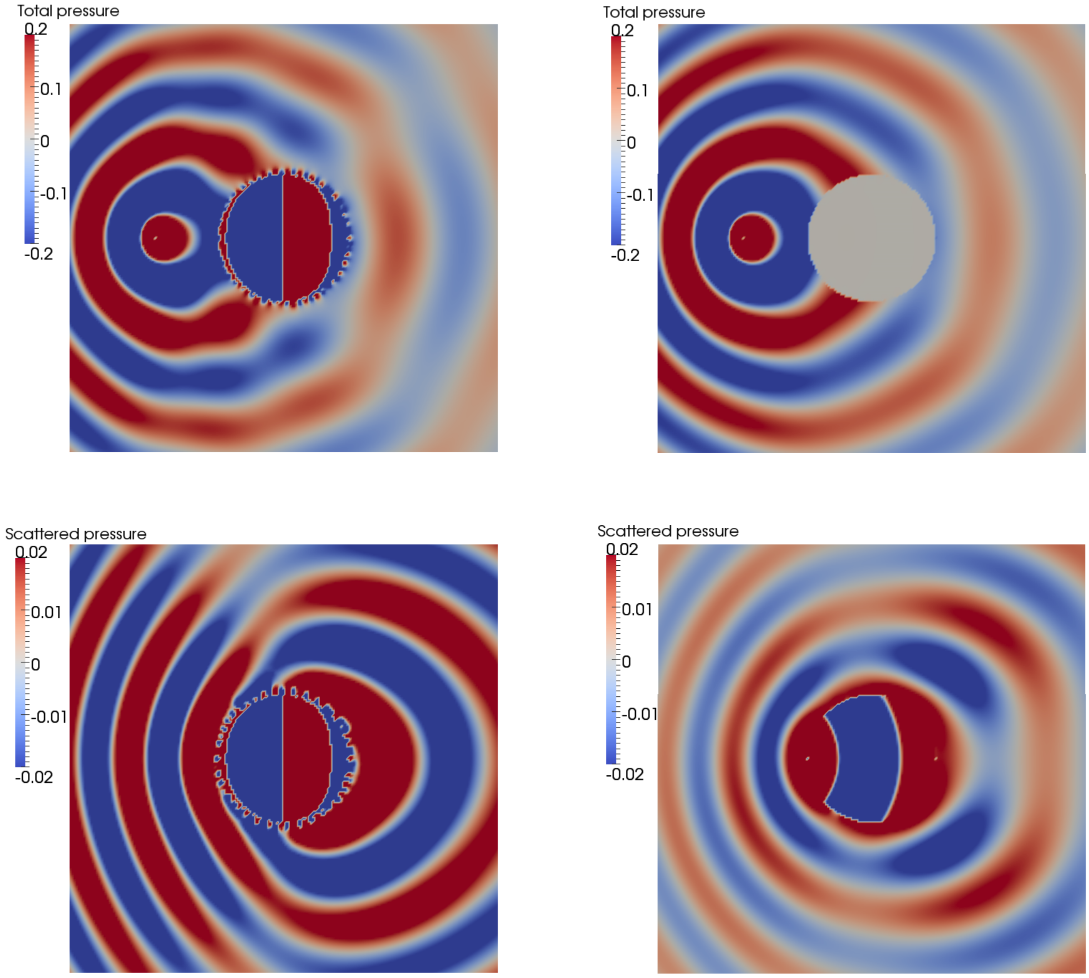

Figure 4: Mesh 1, 1509.849 Hz. Top : real part of the total pressure; left: unstable formulation (30), right: stable formulation (39). Bottom : real part of the scattered pressure; left: unstable formulation (30), right: stable formulation (39). At this resonant frequency, the two formulations yield different results.

simulations at higher frequencies.

5.4 Convergence

To further study the impact of the ill-conditioning of the unstable formulation (30) on the computed solution, the preconditioning is not used in what follows. First, the value of the acoustic pressure on a network of 10000 points located further than 0.5 m from the center of the sphere (therefore in Ω^+) is computed using the stable formulation (39) with Mesh 1 at the resonant frequency 1509.849 Hz. This computed acoustic pressure is called the accurate pressure. Next, the acoustic pressure on the same network of points is computed for different values of the number of iterations of the solver, using the unstable formulation (30) and the stable formulation (39) with Mesh 1 at the resonance 1509.849 Hz. The relative difference between the computed pressure and the accurate pressure in Euclidian norm is called the relative error. Figure 7 presents the relative residual and the relative error with respect to the number of iterations. With the unstable formulation (30), the relative residual decreases irregularly. In particular, it stays constant during around 200 iterations. The relative error decreases, stays constant, rises after 400 iterations, and finally stabilizes at a large value, whereas the relative residual keeps converging to zero. As for every ill-conditioned problem, the relative residual cannot be used to ascertain convergence towards the correct solution. In particular, the relative residual is extremely small, while the error is of order one. With the stable formulation (39), the relative residual

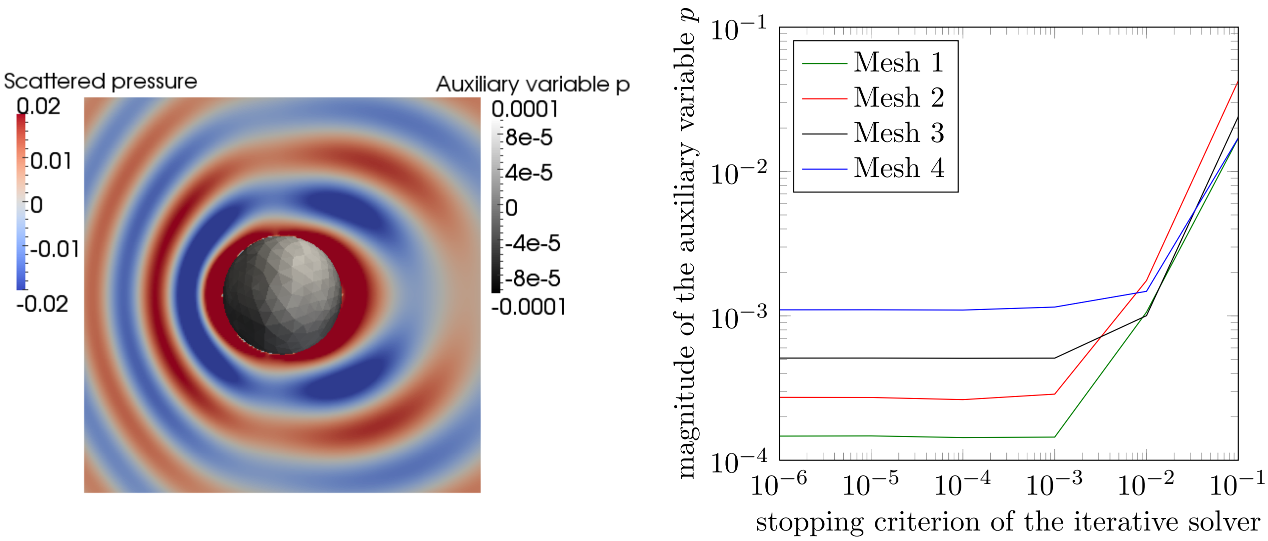

Figure 5: Stable formulation (39) at 1500 Hz. Left : real part of the scattered pressure and auxiliary variable p with Mesh 1. Right : Magnitude of the auxiliary variable p as a function of the stopping criterion of the iterative linear solver with all meshes.

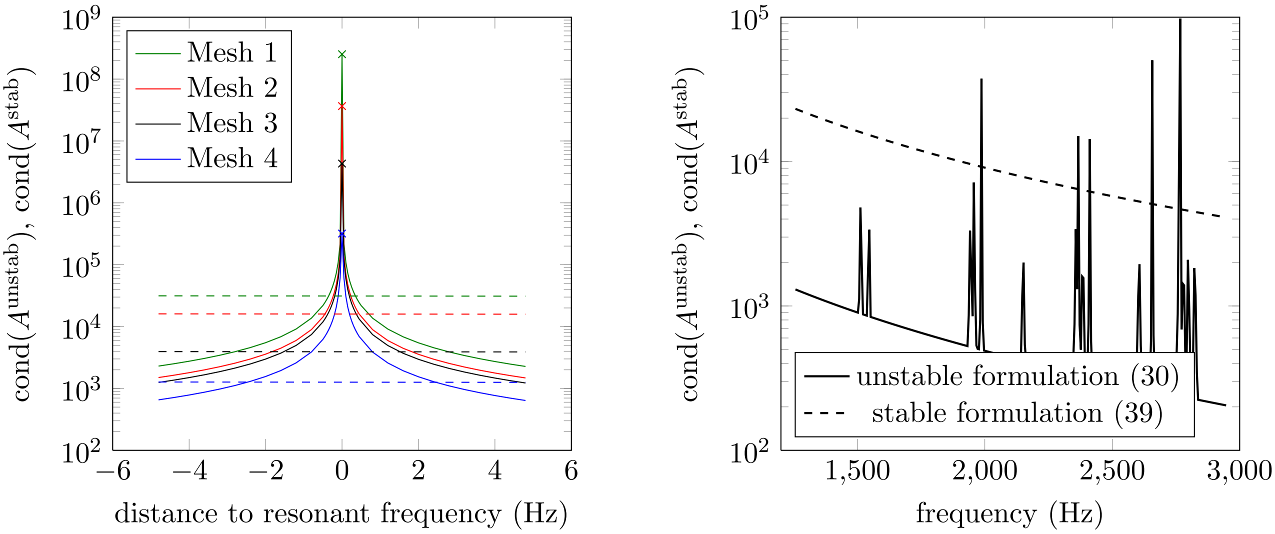

Figure 6: Condition number of the matrix for the unstable formulation (30) (solid) and the stable formulation (39) (dashed). Left: centered representation around a resonant frequency for the four meshes. Right: larger bandwidth with Mesh 2.

and the relative error decrease regularly, and in the same fashion.

5.5 Choice of the coupling parameter η

In the stable formulation (39), the choice of the coupling parameter η is expected to have a direct effect of the condition number of the matrix A^{stab}. In Figure 8, this condition number is plotted for Mesh 4 and for various values of η. For $\eta = 0$, equations (39a)-(39b) are decoupled from (39c), and (39a)-(39b) become (30), so that the curve for $\eta = 0.001$ is similar to the curve of the unstable formulation for Mesh 4 in Figure 6. The condition number appears to be the smallest for η in the range 1 to 10, and worsens for lower and higher values of η. This motivates the choice $\eta = 1$ made in the above simulations.

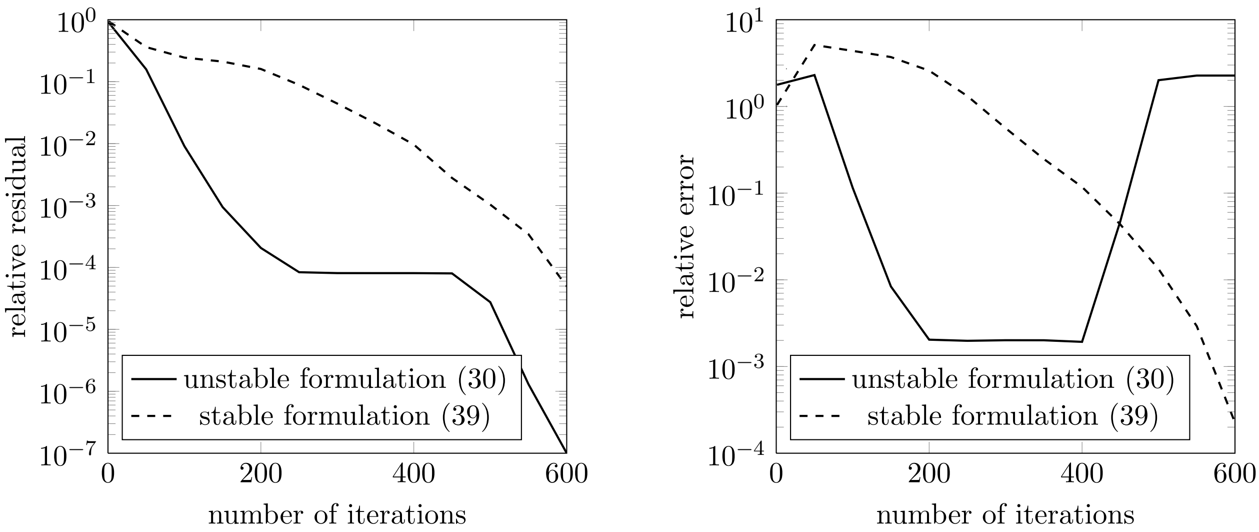

Figure 7: Mesh 1 at resonance 1509.849 Hz; relative residual (left) and relative error (right) with respect to the number of iterations.

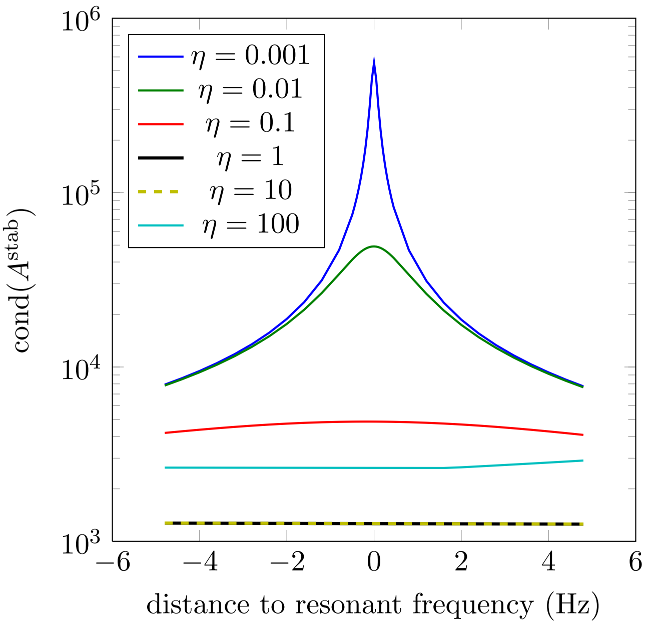

Figure 8: Condition number of the matrix for the stable formulation (39) centered around the resonant frequency at 1535.704 Hz for Mesh 4. In this case, the chosen value $\eta = 1$ leads to the minimal condition numbers.

6 Conclusion

In this work, we derived two coupled boundary element / finite element methods for the convected Helmholtz equation with non-uniform flow in a bounded domain. The first one leads to an unstable formulation, while the second one leads to a stable formulation. The unstable formulation involves two equations and is well-posed except at some resonant frequencies of the source, while the stable one is unconditionally well-posed, but involves three equations. Even if the unstable formulation admits infinitely many solutions at resonant frequencies, the pressure field resulting from any of these solutions equals the one resulting from the stable formulation. However, our numerical results show that at resonant frequencies, the discretization of the unstable formulation is so ill-conditioned that

the pressure field is very different from the one produced by the stable formulation. Moreover, the stable formulation remains tractable within large industrial problems since the relative complexity added by its third equation decreases with the size of the mesh. Its interest is also enhanced by the fact that, at higher frequencies, the density of resonant frequencies is more important.

As long as the uniform flow assumption in the exterior domain is reasonable, more complex flows in the interior domain can be considered, as well as more complex boundary conditions at the surface of the scattering object. These extensions only require to modify the finite element part of the present methodology. An important development for practical simulations is the introduction of modal sources in the interior domain, which is the purpose of [2].

Another interesting extension of this work is the resolution of parametrized aeroacoustic problems, with the frequency of the source as a parameter, using reduced-order models, for instance by means of Proper Generalized Decomposition or Reduced Basis methods. Using the unstable formulation may involve ill-conditioned numerical resolutions if the frequency range of interest contains resonant frequencies, whereas the stable formulation guarantees well-posedness of the procedure. Moreover, the complexity of the online stage of the reduced-order model is not increased by the third equation of the stable formulation.

Acknowledgement

This work was partially supported by EADS Innovation Works. The authors thank Toufic Abboud (IMACS), Nolwenn Balin (EADS Innovation Works), François Dubois (CNAM), Patrick Joly (INRIA), and Tony Lelièvre (CERMICS) for fruitful discussions.

A Derivation of the transformed convected Helmholtz equation (12a)-(12b)

In this appendix, the geometry, unknowns and operators after the Prandtl-Glauert transformation are indicated with primes. To apply this transformation to a PDE in the frequency domain, one has first to change the differential operators as

$$\boldsymbol{\nabla} u = \mathcal{N}\boldsymbol{\nabla}' u, \qquad \boldsymbol{\nabla}\cdot\boldsymbol{U} = \boldsymbol{\nabla}'\cdot\mathcal{N}\boldsymbol{U}, \tag{55}$$

for a scalar-valued function u and a vector-valued function $\boldsymbol{U}$. Here, $\mathcal{N} = I + C_\infty \boldsymbol{M}_\infty \boldsymbol{M}_\infty^T$ with $C_\infty = \frac{\gamma_\infty - 1}{M_\infty^2}$ and $\gamma_\infty = \frac{1}{\sqrt{1-M_\infty^2}}$, and $\boldsymbol{\nabla}'$ refers to derivatives with respect to the transformed variables $\boldsymbol{x}'$. Moreover, it is readily verified that

$$\mathcal{N}\boldsymbol{M} = \boldsymbol{M} + C_\infty P \boldsymbol{M}_\infty, \qquad \mathcal{N}\boldsymbol{M}_\infty = \gamma_\infty \boldsymbol{M}_\infty, \qquad \mathcal{N}\boldsymbol{M}\cdot\boldsymbol{M}_\infty = \mathcal{N}\boldsymbol{M}_\infty\cdot\boldsymbol{M} = \gamma_\infty P, \tag{56}$$

where $P = \boldsymbol{M}\cdot\boldsymbol{M}_\infty$. After changing the differential operators, one has to change the unknown function as $\varphi(\boldsymbol{x}) = \alpha(\boldsymbol{x}')f(\boldsymbol{x}')$, where $\alpha(\boldsymbol{x}') := \exp\left(-ik_\infty\gamma_\infty\left(\boldsymbol{M}_\infty\cdot\boldsymbol{x}'\right)\right)$.

We now show that, following the Prandtl–Glauert transformation, Equation (1) becomes

$$rk^2\beta f + irk\boldsymbol{V}\cdot\boldsymbol{\nabla}' f + \boldsymbol{\nabla}'\cdot\left(irkf\boldsymbol{V} + r\Xi\boldsymbol{\nabla}' f\right) = \varsigma, \tag{57}$$

where $r = \frac{\rho}{\rho_\infty}$, $\beta = (1+qP)^2 - q^2M_\infty^2$, $\boldsymbol{V} = (1+qP)\mathcal{N}\boldsymbol{M} - q\gamma_\infty\boldsymbol{M}_\infty$, $q = \gamma_\infty^2\frac{k_\infty}{k}$, $\Xi = \mathcal{N}(I - \boldsymbol{M}\boldsymbol{M}^T)\mathcal{N}$, and $\varsigma = \rho_\infty^{-1}\alpha^{-1}g$. Dividing Equation (1) by ρ_∞ leads to $\alpha\varsigma = rk^2\varphi + irk\boldsymbol{M}\cdot\boldsymbol{\nabla}'\varphi + \boldsymbol{\nabla}'\cdot\left(r\left(\boldsymbol{\nabla}'\varphi - \left(\boldsymbol{M}\cdot\boldsymbol{\nabla}'\varphi\right)\boldsymbol{M} + ik\varphi\boldsymbol{M}\right)\right)$. Applying (55), it is inferred

$$\alpha\varsigma = rk^2\varphi + irk\boldsymbol{M}\cdot\mathcal{N}\boldsymbol{\nabla}'\varphi + \boldsymbol{\nabla}'\cdot\left(r\mathcal{N}\mathcal{N}\boldsymbol{\nabla}'\varphi\right) - \boldsymbol{\nabla}'\cdot\left(r\left(\boldsymbol{M}\cdot\mathcal{N}\boldsymbol{\nabla}'\varphi\right)\mathcal{N}\boldsymbol{M}\right) + \boldsymbol{\nabla}'\cdot\left(irk\varphi\mathcal{N}\boldsymbol{M}\right).$$

Substituting φ for αf and expanding the derivatives with respect to α yields

$$\begin{aligned}\alpha\varsigma = {} & \alpha rk^2 f + \alpha irk\boldsymbol{M}\cdot\mathcal{N}\boldsymbol{\nabla}' f + \alpha rkk_\infty\gamma_\infty f(\boldsymbol{M}\cdot\mathcal{N}\boldsymbol{M}_\infty) + \boldsymbol{\nabla}'\cdot\left(\alpha r\mathcal{N}\mathcal{N}\boldsymbol{\nabla}' f\right)\\ & - \boldsymbol{\nabla}'\cdot\left(\alpha irk_\infty\gamma_\infty f\mathcal{N}\mathcal{N}\boldsymbol{M}_\infty\right) - \boldsymbol{\nabla}'\cdot\left(\alpha r\left(\boldsymbol{M}\cdot\mathcal{N}\boldsymbol{\nabla}' f\right)\mathcal{N}\boldsymbol{M}\right)\\ & + \boldsymbol{\nabla}'\cdot\left(\alpha irk_\infty\gamma_\infty f\left(\boldsymbol{M}\cdot\mathcal{N}\boldsymbol{M}_\infty\right)\mathcal{N}\boldsymbol{M}\right) + \boldsymbol{\nabla}'\cdot\left(\alpha irkf\mathcal{N}\boldsymbol{M}\right),\end{aligned}$$

since $\boldsymbol{\nabla}'\alpha = -\alpha i k_\infty \gamma_\infty \boldsymbol{M_\infty}$. Using (56) and simplifying some terms leads to

$$\begin{aligned}\alpha\varsigma &= \alpha r k^2 f + \alpha i r k \boldsymbol{M}\cdot\mathcal{N}\boldsymbol{\nabla}' f + \alpha r k^2 q P f + \boldsymbol{\nabla}'\cdot\left(\alpha r \mathcal{N}\mathcal{N}\boldsymbol{\nabla}' f\right) - \boldsymbol{\nabla}'\cdot\left(\alpha i r k \gamma_\infty q f \boldsymbol{M}_\infty\right) \\ &\quad - \boldsymbol{\nabla}'\cdot\left(\alpha r\left(\boldsymbol{M}\cdot\mathcal{N}\boldsymbol{\nabla}' f\right)\mathcal{N}\boldsymbol{M}\right) + \boldsymbol{\nabla}'\cdot\left(\alpha i r k (1+qP) f \mathcal{N}\boldsymbol{M}\right).\end{aligned}$$

Expanding again the derivatives with respect to α yields

$$\begin{aligned}\varsigma &= r k^2 f + i r k \boldsymbol{M}\cdot\mathcal{N}\boldsymbol{\nabla}' f + r k^2 q P f + \boldsymbol{\nabla}'\cdot\left(r\mathcal{N}\mathcal{N}\boldsymbol{\nabla}' f\right) - i r k_\infty \gamma_\infty \mathcal{N}\mathcal{N}\boldsymbol{\nabla}' f\cdot\boldsymbol{M}_\infty \\ &\quad - \boldsymbol{\nabla}'\cdot\left(i r k q \gamma_\infty f \boldsymbol{M}_\infty\right) - r k k_\infty q \gamma_\infty^2 f M_\infty^2 - \boldsymbol{\nabla}'\cdot\left(r\left(\boldsymbol{M}\cdot\mathcal{N}\boldsymbol{\nabla}' f\right)\mathcal{N}\boldsymbol{M}\right) \\ &\quad + i r k_\infty \gamma_\infty \left(\boldsymbol{M}\cdot\mathcal{N}\boldsymbol{\nabla}' f\right)\mathcal{N}\boldsymbol{M}\cdot\boldsymbol{M}_\infty + \boldsymbol{\nabla}'\cdot\left(i r k (1+qP) f \mathcal{N}\boldsymbol{M}\right) + r k k_\infty \gamma_\infty (1+qP) f \mathcal{N}\boldsymbol{M}\cdot\boldsymbol{M}_\infty.\end{aligned}$$

Using again (56) as well as the symmetry of $\mathcal{N}$, it is inferred

$$\begin{aligned}\varsigma &= r k^2 f + i r k \mathcal{N}\boldsymbol{M}\cdot\boldsymbol{\nabla}' f + r k^2 q P f + \boldsymbol{\nabla}'\cdot\left(r\mathcal{N}\mathcal{N}\boldsymbol{\nabla}' f\right) - i r k q \gamma_\infty \boldsymbol{M}_\infty\cdot\boldsymbol{\nabla}' f \\ &\quad - \boldsymbol{\nabla}'\cdot\left(i r k q \gamma_\infty f \boldsymbol{M}_\infty\right) - r k^2 q^2 M_\infty^2 f - \boldsymbol{\nabla}'\cdot\left(r\left(\mathcal{N}\boldsymbol{M}\boldsymbol{M}^T\mathcal{N}\right)\nabla' f\right) \\ &\quad + i r k q P \mathcal{N}\boldsymbol{M}\cdot\boldsymbol{\nabla}' f + \boldsymbol{\nabla}'\cdot\left(i r k (1+qP) f \mathcal{N}\boldsymbol{M}\right) + r k^2 q P (1+qP) f.\end{aligned} \tag{58}$$

The terms are now reorganized with respect to the orders of derivation of f to obtain

$$\begin{aligned}\varsigma &= r k^2 (1 + qP - q^2 M_\infty^2 + qP(1+qP)) f \\ &\quad + i r k \left((1+qP)\mathcal{N}\boldsymbol{M} - q\gamma_\infty \boldsymbol{M}_\infty\right)\cdot\boldsymbol{\nabla}' f \\ &\quad + \boldsymbol{\nabla}'\cdot\left(i r k f \left((1+qP)\mathcal{N}\boldsymbol{M} - q\gamma_\infty \boldsymbol{M}_\infty\right)\right) \\ &\quad + \boldsymbol{\nabla}'\cdot\left(r\mathcal{N}\mathcal{N}\boldsymbol{\nabla}' f\right) - \boldsymbol{\nabla}'\cdot\left(r\left(\mathcal{N}\boldsymbol{M}\boldsymbol{M}^T\mathcal{N}\right)\boldsymbol{\nabla}' f\right),\end{aligned} \tag{59}$$

yielding (57).

We now show that, following the Prandtl–Glauert transformation, the boundary condition (2) becomes

$$\left(i r k f \boldsymbol{V} + r\Xi\boldsymbol{\nabla}' f\right)\cdot\boldsymbol{n}' = 0 \quad \text{on } \Gamma', \tag{60}$$

where Γ' denotes the transformed boundary Γ. The normals on the initial geometry are denoted by $\boldsymbol{n}$, and the normals on the transformed geometry by $\boldsymbol{n}'$. It is readily seen that

$$\boldsymbol{n} = K_\infty \mathcal{N}\boldsymbol{n}' \quad \text{on } \Gamma, \tag{61}$$

where K_∞ is a normalization factor that is not needed in what follows. Owing to (55) and (61), (2) becomes $\mathcal{N}\boldsymbol{\nabla}'\varphi\cdot\mathcal{N}\boldsymbol{n}' = 0$. Hence, $\mathcal{N}\boldsymbol{\nabla}'(\alpha f)\cdot\mathcal{N}\boldsymbol{n}' = 0$, leading to $(\mathcal{N}\boldsymbol{\nabla}' f - i k_\infty \gamma_\infty f \mathcal{N}\boldsymbol{M}_\infty)\cdot\mathcal{N}\boldsymbol{n}' = 0$. Since the flow is tangential on Γ, $\boldsymbol{M}\cdot\boldsymbol{n} = 0$ on Γ. Hence, $\boldsymbol{M}\cdot\mathcal{N}\boldsymbol{n}' = 0$ on Γ, so that

$$\left(\mathcal{N}\boldsymbol{\nabla}' f - \left(\mathcal{N}\boldsymbol{M}\cdot\boldsymbol{\nabla}' f\right)\boldsymbol{M} + i k f \left((1+qP)\boldsymbol{M} - \frac{k_\infty}{k}\gamma_\infty \mathcal{N}\boldsymbol{M}_\infty\right)\right)\cdot\mathcal{N}\boldsymbol{n}' = 0. \tag{62}$$

Using the symmetry of $\mathcal{N}$ and (56), (62) leads to (60).

B Proofs

As preliminary results, we first derive Propositions B.1 and B.2. Then, recalling that (14) is the original transmission problem, (30) the unstable formulation, and (39) the stable formulation, the mathematical results are obtained in the following order:

$$\text{Proposition B.2} \Longrightarrow \begin{cases}\text{Link between (14) and (39) (Proposition 3.9)} \\ \text{Link between (14) and (30) (Proposition 3.5)}\end{cases}$$

$$\Downarrow$$

$$\text{Proposition B.1} \Longrightarrow \begin{cases}\text{Uniqueness for (39)} \Longrightarrow \text{Well-posedness of (39) (Theorem 3.10)} \\ \qquad\qquad \Longrightarrow \text{Well-posedness of (14) (Theorem 3.2)} \\ \text{Conditional uniqueness for (30)} \Longrightarrow \text{Conditional well-posedness of (30)} \\ \qquad\qquad \text{(Theorem 3.7)}\end{cases}$$

Notice that we do no start with the well-posedness of (14) since, to our knowledge, a result directly applicable to it is not available in the literature. Herein, we prove the well-posedness of (39) which is equivalent to (14).

Proposition B.1. *Problem* (14) *has at most one solution in* $H^1_{\text{loc}}(\Omega)$.

Proof. Let $f \in H^1_{\text{loc}}(\Omega)$ solve (14) with $\varsigma = 0$ (so that $f_{\text{inc}} = 0$). From Proposition 3.1, f solves (12). Let B be a ball containing Ω^-. Let $f^t \in H(\Delta, B)$. Using Green's first identity,

$$\begin{aligned} 0 &= \int_{\Omega\cap B} \left(-rk^2\beta\overline{f} - ikr\boldsymbol{V}\cdot\boldsymbol{\nabla}\overline{f} - \boldsymbol{\nabla}\cdot\left(irk\overline{f}\boldsymbol{V} + (r\Xi\boldsymbol{\nabla}\overline{f})\right)\right) f^t \\ &= \int_{\Omega\cap B} r\Xi\boldsymbol{\nabla}\overline{f}\cdot\boldsymbol{\nabla}f^t - rk^2\beta\overline{f}f^t - ikr\boldsymbol{V}\cdot(\boldsymbol{\nabla}\overline{f}f^t - \boldsymbol{\nabla}f^t\overline{f}) - \left(\gamma^-_{1,\partial B}f, \gamma^-_{0,\partial B}f^t\right)_{\partial B}, \end{aligned} \tag{63}$$

where $\gamma^-_{0,\partial B}$ and $\gamma^-_{1,\partial B}$ are the Dirichlet and Neumann traces on ∂B from B. Taking $f^t = f$ yields

$$\left(\gamma^-_{1,\partial B}f, \gamma^-_{0,\partial B}f\right)_{\partial B} = \int_{\Omega\cap B} r\Xi\boldsymbol{\nabla}\overline{f}\cdot\boldsymbol{\nabla}f - rk^2\beta\overline{f}f - 2kr\boldsymbol{V}\cdot\left(\text{Im}\boldsymbol{\nabla}\overline{f}f\right), \tag{64}$$

so that $\text{Im}\left(\gamma^-_{1,\partial B}f, \gamma^-_{0,\partial B}f\right)_{\partial B} = 0$. Using Rellich Lemma (see [31, Lemma 9.9]), since $f \in H^1_{\text{loc}}(\mathbb{R}^3\backslash B)$ solves the classical Helmholtz equation in $\mathbb{R}^3\backslash B$ and satisfies the Sommerfeld radiation condition, as well as $\text{Im}\left(\gamma^-_{1,\partial B}f, \gamma^-_{0,\partial B}f\right)_{\partial B} \geq 0$, it is inferred that $f|_{\mathbb{R}^3\backslash B} \equiv 0$. Equation (6) can be written

$$L(f) := \left(rk^2\beta + \boldsymbol{\nabla}\cdot(irk\boldsymbol{V})\right)f + 2irk\boldsymbol{V}\cdot\boldsymbol{\nabla}f + \boldsymbol{\nabla}\cdot(r\Xi\boldsymbol{\nabla}f) = 0 \quad \text{in } \Omega. \tag{65}$$

From [18, Theorem 1.1], since $r\Xi$ is uniformly elliptic with Lipschitz continuous coefficients, and $rk^2\beta + \boldsymbol{\nabla}\cdot(irk\boldsymbol{V})$ and $2irk\boldsymbol{V}$ have bounded coefficients, the differential operator L satisfies the strong unique continuation property in Ω. Hence, $f|_{\mathbb{R}^3\backslash B} \equiv 0$ implies that the only $H^1_{\text{loc}}(\Omega)$ solution of (12) with $\varsigma = 0$ is $f \equiv 0$ in Ω. The assertion follows from Proposition 3.1. $\square$

Proposition B.2. *Let* (Φ, λ, p) *solve* (39). *There holds* $p = 0$, $\lambda = \gamma_1^-\Phi$, *and*

$$\begin{aligned} rk^2\beta\Phi^- + irk\boldsymbol{V}\cdot\boldsymbol{\nabla}\Phi^- + \boldsymbol{\nabla}\cdot\left(irk\Phi^-\boldsymbol{V} + r\Xi\boldsymbol{\nabla}\Phi^-\right) &= 0 && \text{in } L^2(\Omega^-), && \text{(66a)} \\ \gamma^-_{n,\Gamma}\left(irk\Phi\boldsymbol{V} + r\Xi\boldsymbol{\nabla}\Phi\right) &= 0 && \text{in } H^{-\frac{1}{2}}(\Gamma), && \text{(66b)} \\ N(\gamma_0^-\Phi) + \left(\tilde{D} + \frac{1}{2}I\right)(\lambda) &= \gamma_1 f_{\text{inc}} && \text{in } H^{-\frac{1}{2}}(\Gamma_\infty), && \text{(66c)} \\ \left(D - \frac{1}{2}I\right)(\gamma_0^-\Phi) - S(\lambda) &= -\gamma_0 f_{\text{inc}} && \text{in } H^{\frac{1}{2}}(\Gamma_\infty). && \text{(66d)} \end{aligned}$$

Proof. Set $\boldsymbol{\sigma} := irk\Phi\boldsymbol{V} + r\Xi\boldsymbol{\nabla}\Phi$. Owing to (39a) and recalling the definition (23) of $\mathcal{V}$, there holds, $\forall\Phi^t \in H^1(\Omega^-)$,

$$\int_{\Omega^-} \overline{\boldsymbol{\sigma}}\cdot\boldsymbol{\nabla}\Phi^t = \int_{\Omega^-} rk^2\beta\overline{\Phi}\Phi^t + i\int_{\Omega^-} rk\boldsymbol{V}\cdot\boldsymbol{\nabla}\overline{\Phi}\Phi^t - \left(N(\gamma_0^-\Phi) + \left(\tilde{D} - \frac{1}{2}I\right)(\lambda) - \gamma_1 f_{\text{inc}}, \gamma_0^-\Phi^t\right)_{\Gamma_\infty}. \tag{67}$$

Restricting the test function Φ^t to $C^\infty_c(\Omega^-)$ shows that (66a) holds in $L^2(\Omega^-)$. Moreover, since

$$\int_{\Omega^-} \overline{\boldsymbol{\sigma}}\cdot\boldsymbol{\nabla}\Phi^t = -\int_{\Omega^-} (\boldsymbol{\nabla}\cdot\overline{\boldsymbol{\sigma}})\,\Phi^t + \left(\gamma_n^-\boldsymbol{\sigma}, \gamma_0^-\Phi^t\right)_{\Gamma_\infty} + \left(\gamma^-_{n,\Gamma}\boldsymbol{\sigma}, \gamma^-_{0,\Gamma}\Phi^t\right)_\Gamma, \tag{68}$$

and recalling that $\gamma_n^-\boldsymbol{\sigma} = \gamma_1^-\Phi$ on Γ_∞, owing to the property of the convective flow at Γ_∞,

$$\left(N(\gamma_0^-\Phi) + \left(\tilde{D} - \frac{1}{2}I\right)(\lambda) - \gamma_1 f_{\text{inc}}, \gamma_0^-\Phi^t\right)_{\Gamma_\infty} + \left(\gamma_1^-\Phi, \gamma_0^-\Phi^t\right)_{\Gamma_\infty} + \left(\gamma^-_{n,\Gamma}\boldsymbol{\sigma}, \gamma^-_{0,\Gamma}\Phi^t\right)_\Gamma = 0. \tag{69}$$

Then, by the surjectivity of the trace operators γ_0^- from $H^1(\Omega^-)$ onto $H^{\frac{1}{2}}(\Gamma_\infty)$ and $\gamma_{0,\Gamma}^-$ from $H^1(\Omega^-)$ onto $H^{\frac{1}{2}}(\Gamma)$ (see [35, Theorem 2.6.11]), it is deduced from (69) that (66b) holds, and from (69) and (39b) respectively that

$$N(\gamma_0^-\Phi) + \left(\tilde{D} - \frac{1}{2}I\right)(\lambda) + \gamma_1^-\Phi = \gamma_1 f_{\mathrm{inc}}, \tag{70a}$$

$$\left(D - \frac{1}{2}I\right)(\gamma_0^-\Phi) - S(\lambda) - i\eta p = -\gamma_0 f_{\mathrm{inc}}. \tag{70b}$$

Owing to (39c) and (70a), it is inferred that $\delta_{\Gamma_\infty}(p, p^t) = (\lambda - \gamma_1^-\Phi, p^t)_{\Gamma_\infty}$ for all $p^t \in H^1(\Omega^-)$. From the definition (32) of M, there holds $p = M(\lambda - \gamma_1^-\Phi)$. Let $x := \lambda - \gamma_1^-\Phi$. Then, from (19), (70) can be written

$$\begin{pmatrix} \frac{1}{2}I - D & S \\ N & \frac{1}{2}I + \tilde{D} \end{pmatrix} \begin{pmatrix} \gamma_0^-\Phi \\ \lambda \end{pmatrix} = \begin{pmatrix} -i\eta Mx + \gamma_0 f_{\mathrm{inc}} \\ x + \gamma_1 f_{\mathrm{inc}} \end{pmatrix}, \tag{71}$$

so that $(-i\eta Mx + \gamma_0 f_{\mathrm{inc}}, x + \gamma_1 f_{\mathrm{inc}})$ belongs to the range of the block operator defined in the left-hand side of (71). Under this condition, from [22, Theorem 4.1], citing [39], a radiating piecewise Helmholtz solution u such that $\gamma_0^- u = -i\eta Mx + \gamma_0 f_{\mathrm{inc}}$ and $\gamma_1^- u = x + \gamma_1 f_{\mathrm{inc}}$ can be constructed. Consider v such that $v|_{\Omega^+} = 0$ and $v|_{\mathbb{R}^3\backslash\Omega^+} = u|_{\Omega^-}$, and w such that $w|_{\Omega^+} = 0$ and $w|_{\mathbb{R}^3\backslash\Omega^+} = f_{\mathrm{inc}}$. Since v and w are radiating piecewise Helmholtz solutions, $\hat{u} := v - w$ is also a radiating piecewise Helmholtz solution. Since $[\gamma_0\hat{u}] = i\eta Mx$ and $[\gamma_1\hat{u}] = -x$, (19) implies

$$\begin{pmatrix} \frac{1}{2}I - D & S \\ N & \frac{1}{2}I + \tilde{D} \end{pmatrix} \begin{pmatrix} i\eta Mx \\ -x \end{pmatrix} = \begin{pmatrix} i\eta Mx \\ -x \end{pmatrix}. \tag{72}$$

Consider now $\tilde{u} := \mathcal{S}(x) + \mathcal{D}(i\eta Mx)$. From [25, p. 113], the single-layer and double-layer potentials are radiating piecewise Helmholtz solutions. In particular, $\tilde{u}|_{\mathbb{R}^3\backslash\Omega^+}$ solves the Helmholtz equation in $\mathbb{R}^3\backslash\Omega^+$, therefore

$$\left(\gamma_1^-\tilde{u}^-, \gamma_0^-\tilde{u}^-\right)_{\Gamma_\infty} = \int_{\mathbb{R}^3\backslash\Omega^+} \{|\boldsymbol{\nabla}\tilde{u}|^2 - \hat{k}_\infty^2 |\tilde{u}|^2\} \in \mathbb{R}. \tag{73}$$

From the trace relations (18), there holds $\gamma_0^-\tilde{u}^- = \gamma_0^-(\mathcal{S}(x) + \mathcal{D}(i\eta Mx)) = Sx + i\eta\left(D - \frac{1}{2}\right)Mx$. Then, using the first line of (72), $\gamma_0^-\tilde{u}^- = -i\eta Mx$. Likewise, $\gamma_1^-\tilde{u}^- = x$. From (73), $-i\eta\,(x, Mx)_{\Gamma_\infty} \in \mathbb{R}$. However, since $(x, Mx)_{\Gamma_\infty} = \|Mx\|^2_{H^1(\Gamma_\infty)} \in \mathbb{R}$ and $\mathrm{Re}(\eta) \neq 0$, there holds $(x, Mx)_{\Gamma_\infty} = 0$. Therefore $x = 0$, and $p = Mx = 0$, leading to $\lambda = \gamma_1^-\Phi$. Finally, (66c)-(66d) are directly obtained from (70a)-(70b) using $\lambda = \gamma_1^-\Phi$ and $p = 0$. □

Proof B.3 (Proposition 3.9)**.**

The first part of the proposition is clear from the results of Section 3. Let (Φ, λ, p) solve (39). Since the single-layer and double-layer potentials are radiating piecewise Helmholtz solutions, $\mathcal{R}(\Phi, \lambda)$ satisfies (14b) and (14f). From Proposition B.2, $p = 0$, $\lambda = \gamma_1^-\Phi$, and (66) holds. (14a) and (14c) are just (66a) and (66b). Then, using the definition of $\mathcal{R}$ given in Proposition 3.5 and the trace identities (18), the exterior Dirichlet trace of $\mathcal{R}(\Phi, \lambda)$ is $\gamma_0^+\mathcal{R}(\Phi, \lambda) = \gamma_0^+(-\mathcal{S}(\lambda) + \mathcal{D}(\gamma_0^-\Phi) + f_{\mathrm{inc}}) = -S(\lambda) + (D + \frac{1}{2}I)(\gamma_0^-\Phi) + \gamma_0 f_{\mathrm{inc}}$. Using (66d), there holds $\gamma_0^+\mathcal{R}(\Phi, \lambda) = \gamma_0^-\Phi$, which is $\gamma_0^-\mathcal{R}(\Phi, \lambda)$, from which we infer that the first transmission condition (14d) holds. The second transmission condition (14e) is obtained in the same fashion from the exterior Neumann trace of $\mathcal{R}(\Phi, \lambda)$, (66c), and using the fact that $\lambda = \gamma_1^-\Phi$.

Proposition B.4. *Problem* (39) *has at most one solution.*

Proof. Let (Φ, λ, p) solve (39) with $\gamma_0 f_{\mathrm{inc}} = 0$ and $\gamma_1 f_{\mathrm{inc}} = 0$. From Proposition B.2, $p = 0$ and $\lambda = \gamma_1^-\Phi$. From Proposition 3.9, $\mathcal{R}(\Phi, \lambda)$ solves (14). From the mapping properties of $\mathcal{S}$ and $\mathcal{D}$ (Section 3.2.1), $\mathcal{R}(\Phi, \lambda) \in H^1_{\mathrm{loc}}(\Omega^+ \cup \Omega^-)$. Then, from the transmission conditions (14d) and (14e), $\mathcal{R}(\Phi, \lambda) \in H^1_{\mathrm{loc}}(\Omega)$. Then, Proposition B.1 implies that $\mathcal{R}(\Phi, \lambda) = 0$ in Ω. As a result, there holds $\Phi = \mathcal{R}(\Phi, \lambda)|_{\Omega^-} = 0$, and $\lambda = \gamma_1^-\Phi = 0$. □

Proof B.5 (Theorem 3.10).

Consider the two sesquilinear forms a_1 and a_2 on $\mathbb{H} \times \mathbb{H}$ such that

$$
\begin{aligned}
a_1\left((\Phi, \lambda, p), \left(\Phi^t, \lambda^t, p^t\right)\right) &:= \int_{\Omega^-} r\Xi \boldsymbol{\nabla}\overline{\Phi} \cdot \boldsymbol{\nabla}\Phi^t + \left(N^0(\gamma_0^-\Phi), \gamma_0^-\Phi^t\right)_{\Gamma_\infty} + \overline{(\lambda^t, S^0(\lambda))_{\Gamma_\infty}} + \delta_{\Gamma_\infty}(p, p^t) \\
&+ \left(\left(\tilde{D}^0 - \frac{1}{2}I\right)(\lambda), \gamma_0^-\Phi^t\right)_{\Gamma_\infty} - \overline{\left(\lambda^t, \left(D^0 - \frac{1}{2}I\right)(\gamma_0^-\Phi)\right)_{\Gamma_\infty}}, \\
a_2\left((\Phi, \lambda, p), \left(\Phi^t, \lambda^t, p^t\right)\right) &:= -\int_{\Omega^-} rk^2\beta\overline{\Phi}\Phi^t + i\int_{\Omega^-} rk\boldsymbol{V} \cdot \left(\overline{\Phi}\boldsymbol{\nabla}\Phi^t - \Phi^t\boldsymbol{\nabla}\overline{\Phi}\right) + \left(\left(N - N^0\right)(\gamma_0^-\Phi), \gamma_0^-\Phi^t\right)_{\Gamma_\infty} \\
&+ \overline{(\lambda^t, (S - S^0)(\lambda))_{\Gamma_\infty}} + \left(\left(\tilde{D} - \tilde{D}^0\right)(\lambda), \gamma_0^-\Phi^t\right)_{\Gamma_\infty} - \overline{(\lambda^t, (D - D^0)(\gamma_0^-\Phi))_{\Gamma_\infty}} - i\overline{\eta}\overline{(\lambda^t, p)_{\Gamma_\infty}} \\
&- \left(N(\gamma_0^-\Phi), p^t\right)_{\Gamma_\infty} - \left(\left(\tilde{D} + \frac{1}{2}I\right)(\lambda), p^t\right)_{\Gamma_\infty},
\end{aligned}
\tag{74}
$$

where S^0, D^0, $\tilde{D}^0$ and N^0 are the boundary integral operators S, D, $\tilde{D}$ and N for $\hat{k}_\infty = 0$. Consider the linear form b on $\mathbb{H}$ such that

$$
b\left(\Phi^t, \lambda^t, p^t\right) := \left(\gamma_1 f_{\mathrm{inc}}, \gamma_0^-\Phi^t\right)_{\Gamma_\infty} + \overline{(\lambda^t, \gamma_0 f_{\mathrm{inc}})_{\Gamma_\infty}} - \left(\gamma_1 f_{\mathrm{inc}}, p^t\right)_{\Gamma_\infty}. \tag{75}
$$

Problem (39) can then be written: Find $(\Phi, \lambda, p) \in \mathbb{H}$, such that $\forall\left(\Phi^t, \lambda^t, p^t\right) \in \mathbb{H}$,

$$
a\left((\Phi, \lambda, p), \left(\Phi^t, \lambda^t, p^t\right)\right) = b\left(\Phi^t, \lambda^t, p^t\right), \tag{76}
$$

where $a := a_1 + a_2$. We show the well-posedness of (76) by proving successively that (i) a_1 and a_2 are bounded on $\mathbb{H} \times \mathbb{H}$ and b is bounded on $\mathbb{H}$, (ii) a_1 is $\mathbb{H}$-coercive, (iii) the linear map associated with a_2 is compact from $\mathbb{H}$ into $\mathbb{H}$. With the uniqueness of the solution (Proposition B.4), the assertion follows by the Fredholm alternative.

(i) From Section 2.4, $\Xi\boldsymbol{\nabla}\overline{\Phi} \cdot \boldsymbol{\nabla}\Phi^t \leq \frac{1+M_0^2}{1-M_\infty^2}\|\boldsymbol{\nabla}\overline{\Phi}\|\|\boldsymbol{\nabla}\Phi^t\|$. Then,

$$
\left|\int_{\Omega^-} r\Xi\boldsymbol{\nabla}\overline{\Phi} \cdot \boldsymbol{\nabla}\Phi^t\right| \leq \frac{1}{1 - M_\infty^2}\|r\|_{L^\infty(\Omega^-)}\|1 + M_0^2\|_{L^\infty(\Omega^-)}\|\Phi\|_{H^1(\Omega^-)}\|\Phi^t\|_{H^1(\Omega^-)}. \tag{77}
$$

The other volumic integrals are simply controlled by

$$
\begin{aligned}
\left|\int_{\Omega^-} rk\boldsymbol{V} \cdot \left(\overline{\Phi}\boldsymbol{\nabla}\Phi^t - \Phi^t\boldsymbol{\nabla}\overline{\Phi}\right)\right| &\leq 2\|rk\|_{L^\infty(\Omega^-)}\|\boldsymbol{V}\|_{L^\infty(\Omega^-)^3}\|\Phi\|_{H^1(\Omega^-)}\|\Phi^t\|_{H^1(\Omega^-)}, \\
\left|\int_{\Omega} rk^2\beta\overline{\Phi}\Phi^t\right| &\leq \|rk^2\beta\|_{L^\infty(\Omega^-)}\|\Phi\|_{H^1(\Omega^-)}\|\Phi^t\|_{H^1(\Omega^-)}.
\end{aligned}
\tag{78}
$$

From [31, Theorem 6.11], all the involved integral operators are bounded in their natural trace spaces. The boundedness constant of an operator A is denoted by C_A, and the continuity constant of the interior Dirichlet trace operator is denoted by $C_{\gamma_0^-}$: $\|\gamma_0^-\Phi\|_{H^{\frac{1}{2}}(\Gamma_\infty)} \leq C_{\gamma_0^-}\|\Phi\|_{H^1(\Omega^-)}$. Moreover, since $H^1(\Gamma_\infty) \subset H^{\frac{1}{2}}(\Gamma_\infty)$, there exists a constant $C_{\Gamma_\infty} > 0$ such that $\|p\|_{H^{\frac{1}{2}}(\Gamma_\infty)} \leq C_{\Gamma_\infty}\|p\|_{H^1(\Gamma_\infty)}$. These inequalities lead to

$$
\begin{aligned}
\left|a_1\left((\Phi, \lambda, p), \left(\Phi^t, \lambda^t, p^t\right)\right)\right| &\leq 2\left[1 + \frac{1}{1 - M_\infty^2}\|r\|_{L^\infty(\Omega^-)}\|1 + M_0^2\|_{L^\infty(\Omega^-)} + C_{S^0}\right. \\
&\left.+ C_{\gamma_0^-}\left(1 + C_{D^0} + C_{\tilde{D}^0}\right) + C_{\gamma_0^-}^2 C_{N^0}\right]\|(\Phi, \lambda, p)\|_{\mathbb{H}}\|\left(\Phi^t, \lambda^t, p^t\right)\|_{\mathbb{H}}, \\
\left|a_2\left((\Phi, \lambda, p), \left(\Phi^t, \lambda^t, p^t\right)\right)\right| &\leq 2\left[\|rk^2\beta\|_{L^\infty(\Omega^-)} + 2\|rk\|_{L^\infty(\Omega^-)}\|\boldsymbol{V}\|_{L^\infty(\Omega^-)^3} + C_{\Gamma_\infty}\left(\frac{1}{2} + |\eta| + C_{\tilde{D}}\right) + C_{S^0}\right. \\
&\left.+ C_S + C_{\gamma_0^-}\left(C_{\Gamma_\infty}C_N + C_{D^0} + C_D + C_{\tilde{D}^0} + C_{\tilde{D}}\right) + C_{\gamma_0^-}^2\left(C_{N^0} + C_N\right)\right]\|(\Phi, \lambda, p)\|_{\mathbb{H}}\|\left(\Phi^t, \lambda^t, p^t\right)\|_{\mathbb{H}}, \\
\left|b\left(\Phi^t, \lambda^t, p^t\right)\right| &\leq \sqrt{2}\left((C_{\gamma_0^-} + C_{\Gamma_\infty})\|\gamma_1 f_{\mathrm{inc}}\|_{H^{-\frac{1}{2}}(\Gamma_\infty)} + \|\gamma_0 f_{\mathrm{inc}}\|_{H^{\frac{1}{2}}(\Gamma_\infty)}\right)\|\left(\Phi^t, \lambda^t, p^t\right)\|_{\mathbb{H}}.
\end{aligned}
$$

(ii) Unlike D and $\tilde{D}$, the operators D^0 and $\tilde{D}^0$ are real-valued. They are therefore adjoint, so that

$$\left(\left(\tilde{D}^0 - \frac{1}{2}I\right)(\lambda), \gamma_0^-\Phi\right)_{\Gamma_\infty} - \overline{\left(\lambda, \left(D^0 - \frac{1}{2}I\right)(\gamma_0^-\Phi)\right)_{\Gamma_\infty}} \in i\mathbb{R}. \tag{79}$$

From [11, Theorem 2], the operators N^0 and S^0 are strongly elliptic in their natural trace spaces. Moreover, from Section 2.4, for all $\boldsymbol{U} \in \mathbb{C}^3$, $\overline{\boldsymbol{U}} \cdot \Xi \boldsymbol{U} \geq \left(1 - M_0^2\right) \|\boldsymbol{U}\|^2$. Then, there holds

$$\begin{aligned} \operatorname{Re}\left(a_1\left((\lambda, \Phi, p), (\lambda, \Phi, p)\right)\right) &= \int_\Omega r \Xi \boldsymbol{\nabla}\overline{\Phi} \cdot \boldsymbol{\nabla}\Phi + \left(N^0(\gamma_0^-\Phi), \gamma_0^-\Phi\right)_{\Gamma_\infty} + \overline{(\lambda, S^0(\lambda))_{\Gamma_\infty}} + \delta_{\Gamma_\infty}(p,p) \\ &\geq \inf_{\Omega^-}\left(r\left(1 - M_0^2\right)\right) \|\boldsymbol{\nabla}\Phi\|^2_{L^2(\Omega^-)} + K_{N^0}\|\gamma_0^-\Phi\|^2_{H^{\frac{1}{2}}(\Gamma_\infty)} + K_{S^0}\|\lambda\|^2_{H^{-\frac{1}{2}}(\Gamma_\infty)} + \|p\|^2_{H^1(\Gamma_\infty)}, \end{aligned} \tag{80}$$

where the coercivity constant of an operator A is denoted by K_A. From the Petree–Tartar Lemma [16, Lemma A.38], it can be shown that there exists a constant $C_{\Omega^-} > 0$ such that $\|\Phi\|_{H^1(\Omega^-)} \leq C_{\Omega^-}\left(\|\boldsymbol{\nabla}\Phi\|_{L^2(\Omega^-)^3} + \|\gamma_0^-\Phi\|_{H^{\frac{1}{2}}(\Gamma_\infty)}\right)$. Therefore,

$$\begin{aligned} \operatorname{Re}\left(a_1\left((\lambda, \Phi, p), (\lambda, \Phi, p)\right)\right) \geq& \frac{1}{2C^2_{\Omega^-}} \min\left(\inf_{\Omega^-}\left(r\left(1 - M_0^2\right)\right), K_{N^0}\right) \|\Phi\|^2_{H^1(\Omega^-)} \\ &+ K_{S^0}\|\lambda\|^2_{H^{-\frac{1}{2}}(\Gamma_\infty)} + \|p\|^2_{H^1(\Gamma_\infty)} \\ \geq& \min\left(\frac{\inf_{\Omega^-}\left(r\left(1 - M_0^2\right)\right)}{2C^2_{\Omega^-}}, \frac{K_{N^0}}{2C^2_{\Omega^-}}, K_{S^0}, 1\right) \|\,(\Phi, \lambda, p)\,\|^2_{\mathbb{H}}. \end{aligned} \tag{81}$$

(iii) Let V be a Hilbert space, let A be an operator from V to V, and let a be a sesquilinear form such that, for all $u, v \in V$, $a(u,v) = (Au, v)_V$. A classical result states that A is compact if and only if, for all weakly convergent sequences $(u_n), (v_n) \in V^{\mathbb{N}}$ such that $u_n \rightharpoonup u$ and $v_n \rightharpoonup v$, there holds, up to subsequences, $a(u_n, v_n) \to a(u,v)$. Let $(\Phi_{1n}, \lambda_{1n}, p_{1n}) \rightharpoonup (\Phi_1, \lambda_1, p_1)$ and $(\Phi_{2n}, \lambda_{2n}, p_{1n}) \rightharpoonup (\Phi_2, \lambda_2, p_1)$ be two weakly convergent sequences in $\mathbb{H}$. Since the injection of $H^1(\Omega^-)$ into $L^2(\Omega^-)$ is compact, then, up to subsequences, $\Phi_{in} \to \Phi_i$ and $\boldsymbol{\nabla}\Phi_{in} \rightharpoonup \boldsymbol{\nabla}\Phi_i$, $i = 1, 2$, in $L^2(\Omega^-)$. Therefore, up to subsequences,

$$\begin{aligned} -\int_{\Omega^-} rk^2\beta\overline{\Phi_{1n}}\Phi_{2n} + i\int_{\Omega^-} rk\boldsymbol{V} \cdot \left(\overline{\Phi_{1n}}\boldsymbol{\nabla}\Phi_{2n} - \Phi_{2n}\boldsymbol{\nabla}\overline{\Phi_{1n}}\right) \\ \to -\int_{\Omega^-} rk^2\beta\overline{\Phi_1}\Phi_2 + i\int_{\Omega^-} rk\boldsymbol{V} \cdot \left(\overline{\Phi_1}\boldsymbol{\nabla}\Phi_2 - \Phi_2\boldsymbol{\nabla}\overline{\Phi_1}\right). \end{aligned} \tag{82}$$

Moreover, from [35, Lemma 3.9.8], $S - S^0$, $N - N^0$, $D - D^0$ and $\tilde{D} - \tilde{D}^0$ are compact operators in their natural trace spaces. Hence, up to subsequences, $\left(S - S^0\right)(\lambda_{1n}) \to \left(S - S^0\right)(\lambda_1)$ in $H^{\frac{1}{2}}(\Gamma_\infty)$, and the corresponding results hold for the other boundary integral operators. Since the injection of $H^1(\Gamma_\infty)$ in $H^{\frac{1}{2}}(\Gamma_\infty)$ is compact, then, up to subsequences, $p_{in} \to p_i$ in $H^{\frac{1}{2}}(\Gamma_\infty)$, so that $(\lambda_{2n}, p_{1n})_{\Gamma_\infty} \to (\lambda_2, p_1)_{\Gamma_\infty}$. The last two terms converge as well by continuity of N, γ_0^- and $\tilde{D}$, as well as the strong convergence of p_{2n} in $H^{\frac{1}{2}}(\Gamma_\infty)$ up to subsequences. This concludes the proof.

Proof B.6 (Theorem 3.2)**.**

This a direct consequence of Proposition 3.9 and Theorem 3.10.

Proof B.7 (Proposition 3.5)**.**

The first part of the proposition is clear from the results of Section 3. Let (Φ, λ) solve (30). In the same fashion as in the proof of Proposition B.2, (14a) and (14c) hold, as well as

$$\begin{pmatrix} \frac{1}{2}I + D & -S \\ -N & \frac{1}{2}I - \tilde{D} \end{pmatrix} \begin{pmatrix} \gamma_0^-\Phi \\ \lambda \end{pmatrix} = \begin{pmatrix} \gamma_0^-\Phi \\ \gamma_1^-\Phi \end{pmatrix}, \tag{83}$$

so that $\left(\gamma_0^-\Phi, \gamma_1^-\Phi\right)$ belongs to the range of the block operator defined in the left-hand side of (83). Under this condition, from [22, Theorem 4.1], citing [39], a radiating piecewise Helmholtz solution u such that $\gamma_0^+ u = \gamma_0^-\Phi$ and $\gamma_1^+ u = \gamma_1^-\Phi$ can be constructed. Consider the function v defined as $v|_{\Omega^+} = u|_{\Omega^+}$ and $v|_{\mathbb{R}^3\setminus\Omega^+} = 0$. The function v is still a radiating piecewise Helmholtz solution, and its jumps of traces are $[\gamma_0 v]_{\Gamma_\infty} = \gamma_0^-\Phi$ and $[\gamma_1 v]_{\Gamma_\infty} = \gamma_1^-\Phi$. From (19), $\left(\frac{1}{2}I - D\right)\gamma_0^-\Phi + S\gamma_1^-\Phi = -\gamma_0^- v^- = 0$. Together with the first line of (83), it is deduced that $\lambda - \gamma_1^-\Phi \in \ker(S) = \ker(\tilde{D} - \frac{1}{2}I)$. Therefore, (66c) and (66d) hold. Then, since single-layer and double-layer potentials are radiating piecewise Helmholtz solutions, $\mathcal{R}(\Phi, \lambda)$ satisfies (14b) and (14f). Finally, taking the exterior traces of $\mathcal{R}(\Phi, \lambda)$, the transmission conditions (14d) and (14e) are directly obtained from (66c), (66d) and $\lambda - \gamma_1^-\Phi \in \ker(S) = \ker(\tilde{D} - \frac{1}{2}I)$, in the same fashion as in Proof B.3.

Proof B.8 (Theorem 3.7)**.**

Let (Φ, λ) solve (30) with $\gamma_0 f_{\text{inc}} = 0$ and $\gamma_1 f_{\text{inc}} = 0$. From Proposition 3.5, $\mathcal{R}(\Phi, \lambda)$ solves (14). As seen in Proof B.4, $\mathcal{R}(\Phi, \lambda) \in H^1_{\text{loc}}(\Omega)$. It is then deduced from Proposition B.1 that $\mathcal{R}(\Phi, \lambda) = 0$ in Ω. As a consequence, $\Phi = \mathcal{R}(\Phi, \lambda)|_{\Omega^-} = 0$. From Proof B.7, $\lambda - \gamma_1^-\Phi \in \ker(S)$. Suppose $-\hat{k}_\infty^2 \notin \Lambda$. Then, $\ker(S) = \{0\}$, leading to $\lambda = \gamma_1^-\Phi = 0$, so that problem (30) has at most one solution; well-posedness is then obtained using the Fredholm alternative by proceeding similarly to Proof B.5. Suppose $-\hat{k}_\infty^2 \in \Lambda$. Let $\lambda^* \in \ker(S) = \ker(\tilde{D} - \frac{1}{2}I)$, and f be the solution to (14). From Proposition 3.6, $(f^-, \gamma_1 f + \lambda^*)$ solves (30).

References

[1] R. Amiet and W. R. Sears. The aerodynamic noise of small-perturbation subsonic flows. *Journal of Fluid Mechanics*, (44), 1928.

[2] N. Balin, F. Casenave, F. Dubois, E. Duceau, S. Duprey, and I. Terrasse. Boundary element and finite element coupling for aeroacoustic simulations. In preparation, 2013.

[3] P. Bettess. *Infinite Elements*. Penshaw Press: Cleadon, Sunderland, U.K., 1992.

[4] P. Bettess, D. W. Kelly, and O. C. Zienkiewicz. The coupling of the finite element method and boundary solution procedures. *Int. J. Numer. Meth. Engng.*, 11:355–375.

[5] H. Brakhage and P. Werner. Über das Dirichletsche Außenraum Problem für die Helmholtzsche Schwingungsgleichung. *Arch. der Math.*, 16:325–329, 1965.

[6] S.C. Brenner and L.R. Scott. *The Mathematical Theory of Finite Element Methods*. Texts in Applied Mathematics. Springer, 2008.

[7] A. Buffa and R. Hiptmair. Regularized combined field integral equations. *Numer. Math.*, 100(1):1–19, mar 2005.

[8] B. Carpentieri. *Sparse preconditioners for dense linear systems from electromagnetic applications*. PhD thesis, CERFACS, 2002.

[9] B. Carpentieri, I. Duff, L. Giraud, and G. Sylvand. Combining fast multipole techniques and an approximate inverse preconditioner for large electromagnetism calculations. *SIAM Journal on Scientific Computing*, 27(3):774–792, 2005.

[10] M. Costabel. *Symmetric methods for the coupling of finite elements and boundary elements*. Boundary Elements IX, Vol. 1, Springer-Verlag, Berlin.

[11] M. Costabel. Boundary integral operators on Lipschitz domains: Elementary results. *SIAM Journal on Mathematical Analysis*, 19(3):613–626, 1988.

[12] A. Delnevo and I. Terrasse. Code acti3s harmonique, justification mathématique, Partie I. Technical report, EADS, 2001.

[13] A. Delnevo and I. Terrasse. Code acti3s, justifications mathématiques, Partie II : presence d'un écoulement uniforme. Technical report, EADS, 2002.

[14] F. Dubois, E. Duceau, F. Maréchal, and I. Terrasse. Lorentz transform and staggered finite differences for advective acoustics. Technical report, EADS, 2002.

[15] J. El Gharib. *Méthode des potentiels retardés pour l'acoustique.* PhD thesis, École Polytechnique, 1999.

[16] A. Ern and J.L. Guermond. *Theory and Practice of Finite Elements.* Number vol. 159 in Applied Mathematical Sciences. Springer, 2004.

[17] G. Fairweather, A. Karageorghis, and P.A. Martin. The method of fundamental solutions for scattering and radiation problems. *Engineering Analysis with Boundary Elements*, 27(7):759 – 769, 2003.

[18] N. Garofalo and F.-H. Lin. Unique continuation for elliptic operators: A geometric-variational approach. *Communications on Pure and Applied Mathematics*, 40(3):347–366, 1987.

[19] H. Glauert. The effect of compressibility on the lift of an aerofoil. *Proceedings of the Royal Society of London, Series A*, 118(779):pp. 113–119, 1928.

[20] M.E. Goldstein. *Aeroacoustics.* McGraw-Hill International Book Company, 1976.

[21] M.F. Hamilton and D.T. Blackstock. *Nonlinear Acoustics: Theory and Applications.* Elsevier Science & Tech, 1998.

[22] R. Hiptmair and P. Meury. Stabilized FEM-BEM coupling for Helmholtz transmission problems. *SIAM J. Numer. Anal.*, 44(5):2107–2130, 2006.

[23] A. Hirschberg and S. W. Rienstra. *An Introduction to Acoustics.* Eindhoven University of Technology, 2004.

[24] G. C. Hsiao and W. L. Wendland. *Boundary Element Methods: Foundation and Error Analysis.* John Wiley & Sons, Ltd, 2004.

[25] C. Johnson and J. C. Nédélec. On the coupling of boundary integral and finite element methods. *Mathematics of Computation*, 35(152):pp. 1063–1079, 1980.

[26] J. Langou. *Solving large linear systems with multiple right-hand sides.* PhD thesis, INSA, 2003.

[27] R. Leis. Zur Dirichletschen Randwertaufgabe des Außenraumes der Schwingungsgleichung. *Mathematische Zeitschrift*, 90:205–211, 1965.

[28] V. Levillain. *Couplage éléments finis-équations intégrales pour la résolution des équations de Maxwell en milieu hétèrogène.* PhD thesis, École Polytechnique, 1991.

[29] M. J. Lighthill. On sound generated aerodynamically. I. General theory. *Proceedings of the Royal Society of London. Series A, Mathematical and Physical Sciences*, 211(1107):pp. 564–587, 1952.

[30] M. J. Lighthill. On sound generated aerodynamically. II. Turbulence as a source of sound. *Proceedings of the Royal Society of London. Series A, Mathematical and Physical Sciences*, 222(1148):pp. 1–32, 1954.

[31] W. McLean. *Strongly Elliptic Systems and Boundary Integral Equations.* Cambridge University Press, 2000.

[32] D.P. O'Leary. The block conjugate gradient algorithm and related methods. *Linear Algebra and its Applications*, 29(0):293 – 322, 1980.

[33] O. Panich. On the question of the solvability of the exterior boundary value problems for the wave equation and Maxwell's equations. *Usp. Mat. Nauk.*, 20A:221–226, 1965.

[34] Y. Saad and M. Schultz. GMRES: A generalized minimal residual algorithm for solving non-symmetric linear systems. *SIAM Journal on Scientific and Statistical Computing*, 7(3):856–869, 1986.

[35] S.A. Sauter and C. Schwab. *Boundary Element Methods.* Springer Series in Computational Mathematics. Springer, 2010.

[36] T. Sayah. *Méthodes des potentiels retardés pour les milieux hétérogènes et l'approximation des couches minces par conditions d'impédance généralisées en électromagnétisme.* PhD thesis, École Polytechnique, 1998.

[37] L. Tartar. *An Introduction to Sobolev Spaces and Interpolation Spaces.* Lecture Notes of the Unione Matematica Italiana. Springer, 2007.

[38] J. Utzmann, C.-D. Munz, M. Dumbser, E. Sonnendrücker, S. Salmon, S. Jund, and E. Frénod. *Numerical Simulation of Turbulent Flows and Noise Generation.* Springer, 2009.

[39] T. Von Petersdorff and R. Leis. Boundary integral equations for mixed Dirichlet, Neumann and transmission problems. *Mathematical Methods in the Applied Sciences*, 11(2):185–213, 1989.

[40] O.C. Zienkiewicz and P. Bettess. Dynamic fuid-structure interaction. Numerical modelling of the coupled problem. *In Numerical Methods in Offshore Engineering*, pages 185–194, 1978.